Global and Planetary Change 257 (2026) 105236

Contents lists available at ScienceDirect

Global and Planetary Change

journal homepage: www.elsevier.com/locate/gloplacha

Research Article

Understanding green house gases emission dynamics from forest fires in Thailand using predictive models☆

Fahad Shahzad[a,c,1], Kaleem Mehmood[a,d,*,1], Shoaib Ahmad Anees[e], Muhammad Adnan[f], Khadim Hussain[d], Waseem Razzaq Khan[g], Munawar Shah[h], Punyawi Jamjareegulgarn[i], Manuela Oliveira[b,*], José G. Borges[j]

[a] Precision Forestry Key Laboratory of Beijing, Beijing Forestry University, Beijing 100083, China
[b] Department of Mathematics and Center for Research on Mathematics and its Applications, University of Évora, Évora, Portugal
[c] State Forestry and Grassland Administration Key Laboratory of Forest Resources and Environmental Management, Beijing Forestry University, Beijing 100083, PR China
[d] Institute of Forest Science, University of Swat, Main Campus Charbagh, 19120 Swat, Pakistan
[e] Department of Forestry, The University of Agriculture, Dera Ismail Khan 29050, Pakistan
[f] State Key Laboratory of Resources and Environmental Information System, Institute of Geographic Sciences and Natural Resources Research, CAS, Beijing 100101, China
[g] Department of Forestry Science and Biodiversity, Faculty of Forestry and Environment, University Putra Malaysia, Serdang 43400, Malaysia
[h] Space Education and GNSS Lab, NCGSA, Department of Space Science, Institute of Space Technology, 44000 Islamabad, Pakistan
[i] King Mongkut's Institute of Technology Ladkrabang, Prince of Chumphon Campus, Chumphon 86160, Thailand
[j] Forest Research Centre, TERRA Associate Laboratory, School of Agriculture, University of Lisbon, Tapada da Ajuda, 1349-017 Lisboa, Portugal

ARTICLE INFO

Editor: Dr. Jed O Kaplan

Keywords:
Forest fires
Greenhouse gas emissions
Machine learning
Net primary productivity
Fire management strategies

ABSTRACT

Forest fires are a major driver of carbon emissions, particularly in tropical regions where climate variability and land use practices intensify their frequency and impact. This study investigates the spatiotemporal trends and emission dynamics of forest fires across Thailand's three dominant vegetation types- Evergreen Broadleaf Forest (EBF), Deciduous Broadleaf Forest (DBF), and Grassland over three climatic seasons (Dry, Hot, and Wet) in the period 2001–2023. Using the Mann-Kendall trend test and Sen's Slope estimator, we observed significant declines in burnt area during the Dry season in EBF and Grasslands, with no consistent trend in DBF. Fire–vegetation interactions revealed seasonally specific effects: positive correlations between fire count and Net Primary Productivity (NPP) were detected in the Wet and the hot seasons in the case of DBF and Grasslands, respectively. Emission analysis showed that CO_2 was the dominant greenhouse gas released, with the Dry season contributing to most emissions, although Hot season emissions have increased over time. Machine learning models Random Forest (RF) and eXtreme Gradient Boosting (XGBoost) explained over 78 % of the variance in CO_2 emissions on test data ($R^2 = 0.79$ for RF, 0.78 for XGBoost), despite higher Root Mean Square Error (RMSE) values (~550) on unseen data. The Shapley Additive Explanations (SHAP) analysis identified wind components and solar radiation as key predictive variables. Central, Northeastern, and Northern Thailand emerged as emission hotspots. These findings improve our understanding of emission dynamics from tropical fires and underscore the need for region-specific mitigation strategies to inform carbon inventories and climate policy.

1. Introduction

Biomass burning (BB) is a widespread global phenomenon involving the combustion of organic and vegetative matter from forest and savanna ecosystems, and of agricultural residues (Tripathi et al., 2024). As a major source of trace gases and aerosols, BB significantly influences both local air quality and global climate systems (Kumari et al., 2024; Rovithakis and Voulgarakis, 2024). It ranks among the leading

☆ This article is part of a Special issue entitled: 'Fire' published in Global and Planetary Change.

* Corresponding authors at: Institute of Forest Science, University of Swat, Main Campus Charbagh, 19120 Swat, Pakistan (Kaleem Mehmood).
E-mail addresses: kaleemmehmood55@gmail.com (K. Mehmood), mmo@uevora.pt (M. Oliveira).

[1] These authors contributed equally to this work.

https://doi.org/10.1016/j.gloplacha.2025.105236
Received 7 March 2025; Received in revised form 12 November 2025; Accepted 5 December 2025
Available online 7 December 2025

contributors to primary fine carbonaceous particles and is the second-largest source of trace gases globally, following fossil fuel combustion (Bessagnet et al., 2022; Taweesan et al., 2025). Emissions from BB such as carbon dioxide (CO_2), methane (CH_4), carbon monoxide (CO), sulfur dioxide (SO_2), and nitrogen oxides (NO_x) are key drivers of atmospheric chemical processes, including tropospheric ozone formation and aerosol generation (deRichter and Caillol, 2011; Grutzen and Andreae, 1990; Kanchanaroek et al., 2025; Unger et al., 2006). These processes have particularly strong implications in tropical regions where fire activity is both frequent and intense.

In Southeast Asia, and especially in Thailand, BB is a major emission source that degrades air quality and contributes to global atmospheric change. Thailand's tropical monsoon climate, coupled with land clearing and agricultural residue burning, makes it highly susceptible to recurring biomass fires particularly in the dry season (Moran et al., 2019). The burning of forest biomass, cropland residues, and biofuels used in cooking and small-scale industry remain dominant contributors (Phairuang et al., 2019; J. Chen et al., 2017; Van der Werf et al., 2003). Region-specific studies have further demonstrated that wildfires in northern Thailand intensify during haze seasons, with elevated PM and CO emissions (Aman et al., 2025; Baek et al., 2025). Biomass composition including the proportion of live vs. dead matter, lignin content, and moisture strongly influences the combustion phase and thus the emission profiles of different gases during forest fires. Nonetheless, despite this growing body of research, many emission inventories in Thailand still rely on default global emission factors and generalized vegetation groupings (e.g., GFED or FINN), which may overlook Thailand's unique ecological and combustion regimes (Alaganthiran et al., 2025; Wang et al., 2025). While past studies have leveraged satellite fire products (e.g., MODIS) and global datasets to assess BB (Adam et al., 2021; Yin, 2020; Shi and Yamaguchi, 2014), critical gaps persist in emission factor calibration for Thailand's dominant vegetation types of EBF, DBF, and grasslands. Emission estimates based on African or Australian ecosystems often fail to account for local fire intensity, fuel load, and moisture dynamics (Beringer et al., 2015; Russell-Smith et al., 2021). This highlights the pressing need for locally calibrated BB models and emission inventories that reflect Thailand's forest structure, climatic variability, and land-use practices. The present study addresses this gap by integrating region-specific satellite data, vegetation typologies, and predictive modeling to improve emission estimation accuracy for Thailand's key forest ecosystems.

Thailand's EBFs, DBFs, and grasslands each contribute differently to BB emissions. EBFs, which dominate the country's tropical forest landscape, store significant amounts of carbon but are highly vulnerable to fire-induced carbon loss (Kaewsong et al., 2022). These forests also have longer recovery periods after fire disturbances, limiting their carbon sequestration capacity (Williams et al., 2012). In contrast, DBFs, which are more common in Thailand's drier regions, are more prone to fires due to their seasonal leaf shedding and the availability of fuel during the dry season (Kanjanavanit, 1992). Grasslands, though less biomass-dense, also experience frequent fires that can substantially impact local air quality (Murphy et al., 2023). The variability in fire intensity, from high-temperature forest fires to lower-intensity grass fires, complicates the assessment of BB emissions and their environmental impact. Understanding the combustion characteristics of these vegetation types, including the ratio of flaming to smoldering combustion, is crucial for accurately estimating the emission of gases like CO_2, CO, and CH4 (Ward and Hardy, 1991). However, limited research has specifically addressed fire dynamics in Southeast Asia, especially in Thailand.

Machine learning (ML) has become a transformative tool in environmental science, enabling more accurate and efficient predictions by analyzing large, complex datasets, namely in the case of fires (e.g., Bot and Borges, 2022). ML techniques, such as RF and XGBoost, are particularly effective in modeling and predicting patterns in data with nonlinear relationships, which is common in environmental processes like BB (Bhagat et al., 2021). RF is an ensemble method that combines multiple decision trees to improve accuracy and reduce overfitting, making it ideal for analyzing spatiotemporal data from diverse sources, such as remote sensing imagery from MODIS and Landsat satellites (Y. Zhang et al., 2022). XGBoost, a gradient-boosting algorithm, is known for its high predictive power and efficiency, making it particularly suited for handling large datasets with complex interactions between variables (Bentéjac et al., 2021). In the context of research of BB, ML models can integrate a variety of environmental factors such as climatic, topographic, and population density to predict fire occurrences, estimate BB, and forecast emissions like CO_2, CO, and particulate matter(Littidej et al., 2022; Tiwari et al., 2024). These models can capture the variability of fire intensity across different vegetation types and landscapes, providing a more nuanced understanding of fire dynamics. While ML has been applied globally in fields like vegetation monitoring, its use in BB research and emissions estimation in regions like Southeast Asia, namely Thailand, remains underutilized. Integrating satellite data with ML techniques offers a promising approach to improve emission inventories and generate predictive models of fire behavior, ultimately contributing to more effective fire management and policy decisions (Jain et al., 2020; Bot and Borges, 2022).

Despite growing research on BB, key knowledge gaps persist regarding Thailand's fire-emission dynamics particularly the lack of vegetation- and season-specific emission inventories using regionally calibrated data. NPP, defined as the net carbon gain by vegetation through photosynthesis after subtracting respiration, serves as a proxy for ecosystem productivity and post-fire vegetation recovery. Evaluating NPP alongside fire events allows us to examine fire-ecosystem feedback under seasonal and vegetation-specific contexts. This study addresses these gaps by: (i) quantifying spatiotemporal trends in fire activity and biomass burned across Thailand's three main vegetation types, (ii) analyzing the relationship between fire occurrence and NPP, and (iii) developing and interpreting predictive models of CO_2 emissions using SHAP-enhanced ML techniques. These insights contribute to improved emission inventories and region-specific fire management strategies under a changing climate.

2. Material and methods

2.1. Study area

This study focuses on the Kingdom of Thailand, situated in Southeast Asia on the Indochina Peninsula, with a total land area of approximately 513,000 km^2 and comprising 76 provinces (Jin et al., 2023). Thailand lies between the latitudes of 5°37′N and 20°27′N, and longitudes of 97°22′E and 105°37′E. The country shares borders with Myanmar to the west and north (2202 km), Laos to the northeast and north (1750 km), Cambodia to the east (798 km), and Malaysia to the south (576 km). It is also bordered by the Gulf of Thailand on the southeast and the Andaman Sea on the southwest, with extensive coastlines of 1878 km and 937 km, respectively. The country's landscape is diverse, ranging from lowland plains to rugged mountainous areas. A substantial portion of Thailand's land (around 64 %) lies below 250 m above sea level, though the northern and western regions are characterized by higher elevations, with some mountains reaching up to 2554 m (Talukdar et al., 2024; Mehmood et al., 2025). Thailand is characterized by highland zones concentrated in the north and west regions that are associated with increased forest cover and recurrent fire activity (Fig. 1). This variation in elevation and landscape influences the distribution of ecosystems, which is crucial for understanding the patterns of forest fires. The northern regions, especially the mountainous areas, are densely forested, while the central and southern regions are less forested, with a higher prevalence of agricultural and urban areas.

Thailand's tropical monsoon climate is characterized by three primary seasons: the Dry season (November to March), the Hot season (April–May), and the Wet season (June to October). The southwest monsoon delivers substantial rainfall from May to November, while the

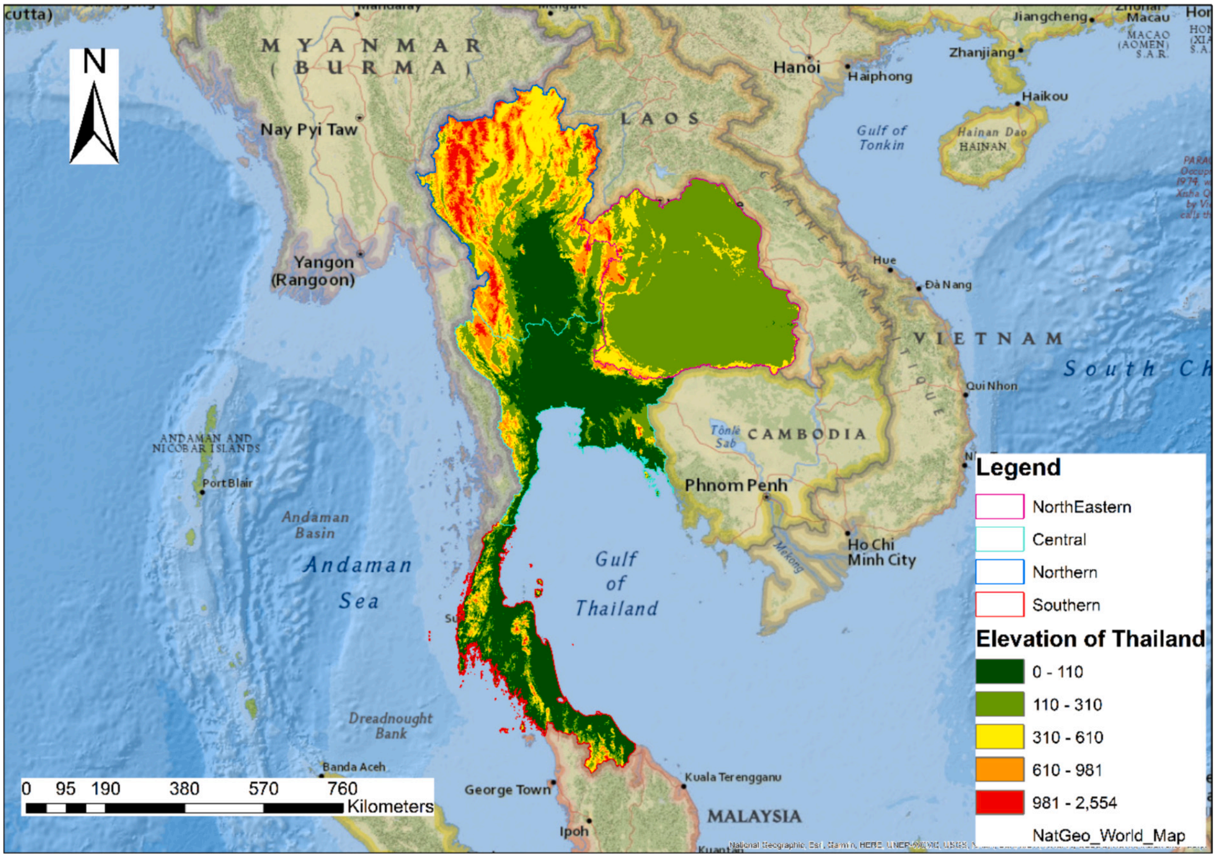

Fig. 1. Elevation map of Thailand overlaid with regional boundaries (Northern, Northeastern, Central, Southern). Elevation ranges from sea level (0 m) to over 2500 m, with higher terrain concentrated in the north and west. This elevational heterogeneity plays a critical role in determining forest type, fire frequency, and emission dynamics across Thailand.

northeast monsoon creates drier conditions from December to April. These seasonal variations directly affect fire activity across the country. Forests cover approximately 32 % of Thailand's total land area and consist mainly of evergreen and deciduous types. Evergreen forests, dominated by *Dipterocarpaceae* species, are largely found in the northern and western regions (Permsirivanchai, 2017). Deciduous forests, including mixed deciduous and Dipterocarp types, are primarily located in the central and eastern regions (Pomoim et al., 2022). The northern and northeastern regions experience the highest frequency of forest fires, particularly during the Dry season (January to April), often influenced by agricultural practices such as slash-and-burn and land clearing. In contrast, the southern region, which has comparatively lower forest cover, experiences fewer fire events, though occasional fires can occur during prolonged dry spells. The varied topography, forest distribution, and seasonal climate conditions result in spatial heterogeneity in fire occurrence across Thailand.

2.2. Forest fire data and processing

This study employs a comprehensive approach to analyze forest fire patterns in Thailand from 2001 to 2023, focusing on fire occurrences and land cover data. The fire spot data (MCD14DL) were sourced from NASA's Fire Information for Resource Management System (FIRMS) (https://firms.modaps.eosdis.nasa.gov/) (Shahzad et al., 2024). The fire spot data, with a spatial resolution of 1 km, includes key parameters such as the time of occurrence, latitude, longitude, and confidence levels (Z. Zhang et al., 2021). Burned area data (MCD64A1), with a spatial resolution of 500 m, represents areas affected by fires that have not yet regenerated into new vegetation (Giglio et al., 2018). This study utilized a grid-based approach to analyze fire events, considering only those with a confidence level exceeding 10 % for detailed analysis (Shahzad et al., 2024). The MCD12Q1 land cover data, also sourced from Google Earth Engine ("MODIS/061/MCD12Q1"), was used to focus on specific vegetation classes in Thailand, including EBF, DBF, and grasslands. The land cover dataset, with a spatial resolution of 500 m, was classified using the LC_Type5 classification, which categorizes land into 12 distinct classes (Hussain et al., 2024; Sulla-Menashe and Friedl, 2018). In addition to fire and land cover datasets, population density was incorporated to account for anthropogenic pressures that influence fire occurrence and spread. Annual gridded population data were sourced from the WorldPop dataset via GEE ("WorldPop/GP/100 m/pop"), resampled to 500 m to match the fire and vegetation datasets. Population density reflects potential ignition sources and land use transitions, particularly near forest-agriculture interfaces. Evaporation, a key indicator of surface moisture and fire susceptibility, was included as a predictor variable to capture eco-climatic variability in fire-prone areas. Monthly evaporation data were obtained from the TerraClimate dataset (Abatzoglou et al., 2018) via GEE at ~4 km resolution and bilinearly resampled to 500 m. Seasonal averages were calculated to align with the fire season classification. Both variables were selected based on prior literature emphasizing their role in fire ignition and fuel dryness. Population density serves as a proxy for human-induced ignition sources, while evaporation reflects surface dryness a critical driver in fire-prone tropical systems. To examine seasonal patterns, the data was divided into Dry, Hot and Wet seasons sub datasets based on the following months: Wry season (November to March), Hot season (April, May) and Wet season (June to October). For each season, the data was processed separately for each vegetation class, ensuring a detailed seasonal and spatial analysis of fire disturbances. Fig. 2 shows a flowchart conceptualizing the main processes.

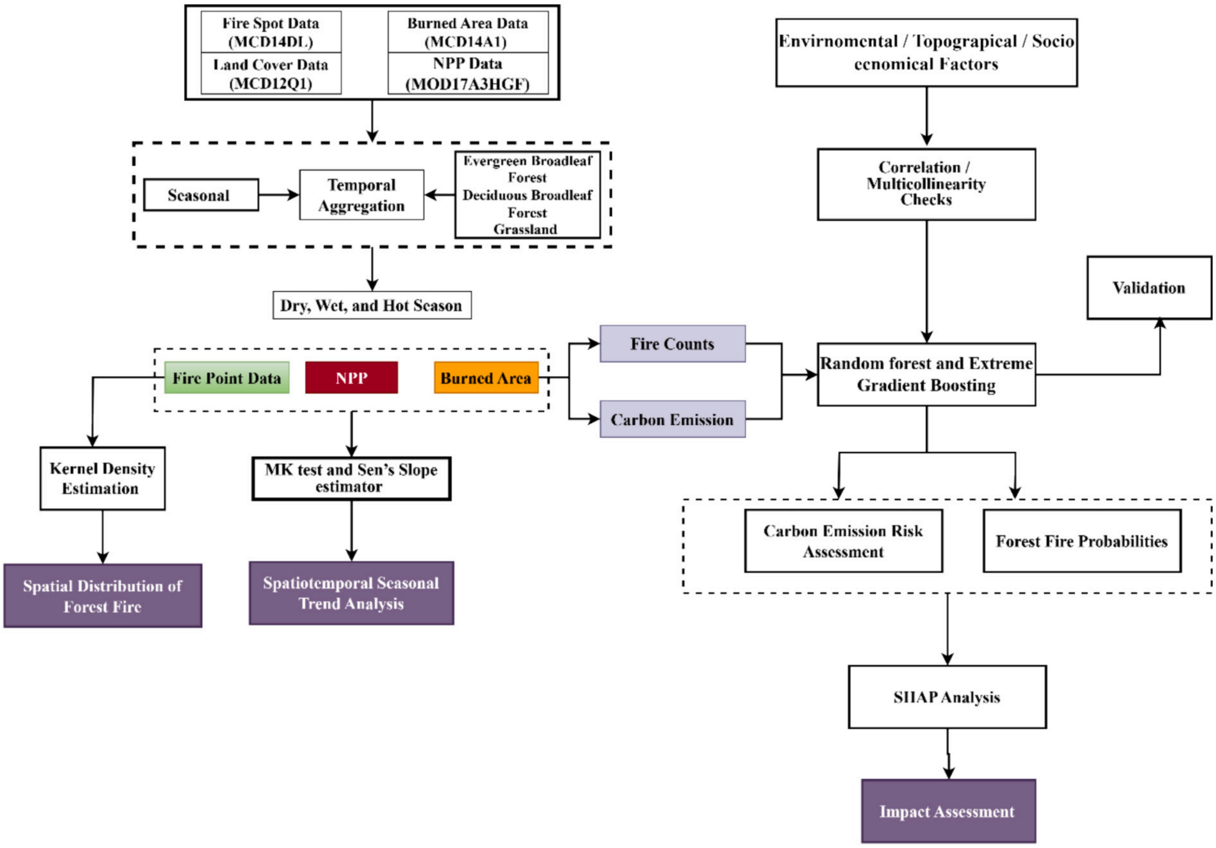

Fig. 2. A conceptual flowchart showing the methodology for the analysis and assessment process.

2.2.1. *Sensitivity analysis of MODIS fire confidence thresholds*

Potential uncertainty from selecting confidence thresholds in MODIS active fire data was addressed through a sensitivity analysis using three widely cited confidence levels: >10 %, >30 %, and > 50 %. While the original analysis employed a > 10 % threshold to ensure inclusive detection of low-intensity fires, especially in surface-level fire regimes such as deciduous forests and grasslands, it is acknowledged that higher thresholds are often recommended for minimizing false positives (Giglio et al., 2018). The MCD14DL fire point dataset was stratified by confidence level, and annual fire counts were computed for each threshold over the 2001–2023 period. These were then compared across time to assess whether the selection of thresholds significantly influenced fire trend patterns. All thresholds were processed consistently using R (*terra, dplyr, ggplot2*) based on point-level fire detection attributes, including acquisition date and confidence scores. Seasonal patterns were also evaluated under the three thresholds to determine whether temporal signatures were sensitive to the threshold choice.

2.3. *NPP data and processing*

The NPP data used in this study were derived from the MOD17-A3HGF product of NASA's EOS/MODIS (MOD17A3HGF.061) for the period 2001–2023. This product provides annual estimates of Gross Primary Production (GPP) and Net Primary Production (NPP) at a 500-m spatial resolution (Mehmood, et al., 2024; Xi et al., 2023). The MOD17A3HGF product is generated at the end of each year, after the complete set of 8-day MOD15A2H data is available, and includes gap-filling to address poor-quality inputs, such as the Leaf Area Index (LAI) and Fraction of Photosynthetically Active Radiation (FPAR). Poor-quality data points are cleaned based on the Quality Control (QC) label, and linear interpolation is applied to any LAI/FPAR pixels that do not meet the quality screening criteria (W. Zhang et al., 2023). The annual GPP and NPP values are derived from the sum of the 8-day GPP Net Photosynthesis (PSN) products (MOD17A2H), where PSN is calculated as the difference between GPP and Maintenance Respiration (MR) (L. Zhang et al., 2019). The data were downloaded in TIFF format from Google Earth Engine, and the original NPP values were converted to kg C/m^2. year by applying a unit conversion factor of 0.0001, by the MOD17A3HGF product requirements. The spatial distribution of mean NPP values across Thailand over the 2001–2023 period highlights productivity gradients tied to forest types and land use zones (Fig. 3). Invalid or outlier values were identified and removed using QGIS to ensure data quality.

2.4. *Calculation of forest biomass burned*

Quantifying total BB is essential for assessing the environmental impact of forest fires. This calculation considers factors such as the burned area, biomass density, and forest burning efficiency, which can vary depending on forest type and seasonal conditions. The total BB was calculated using the following equation (Seiler and Crutzen, 1980):

$$BB = A \times D \times \eta \tag{1}$$

where BB represents the total forest BB (Mg), A is the burned forest area (ha), D is the biomass density per unit area (Mg/ha), and η is the forest burning efficiency. In this study, the biomass densities for different forest types were as follows: EBF (23,350 g/m^2), DBF (20,000 g/m^2), and grassland (1250 g/m^2) (W. Zhang et al., 2023). The forest burning efficiency was set at 25 % for EBF and DBF and grassland at 95 %, based on findings from (Michel et al., 2005) for East Asia. The analysis accounted for Thailand's three distinct seasons Dry, Wet, and Hot. Forest burning patterns were assessed for each season to understand the seasonal variations in fire activity and emissions.

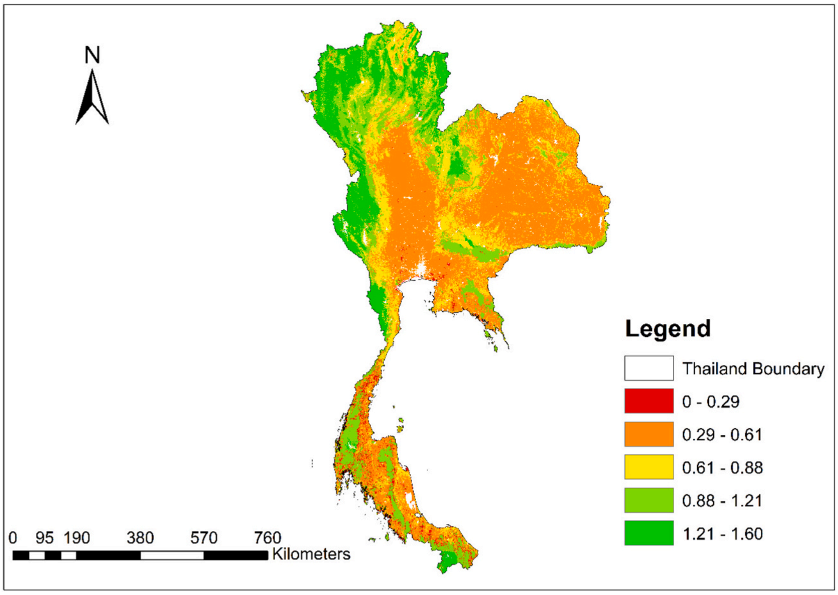

Fig. 3. Mean Net Primary Productivity (NPP) distribution across Thailand from 2001 to 2023, derived from the MOD17A3HGF MODIS product. NPP values (kg C/m^2/year) reveal spatial heterogeneity in ecosystem productivity, with higher productivity (green) concentrated in northern and southern evergreen forest regions, and lower productivity (red/orange) dominant in drier deciduous and agricultural zones of northeastern and central Thailand. (For interpretation of the references to colour in this figure legend, the reader is referred to the web version of this article.)

2.5. Calculation of gaseous emissions from forest biomass burning

In addition to calculating the total BB, it is important to estimate the associated emissions of gases, which contribute to air pollution and climate change. These emissions depend on various factors, including the type of forest burned, the biomass density, and the emission factors for specific gases. The emissions of gases resulting from forest burning were estimated using the following equation (W. Zhang et al., 2023):

$$E_{i,j} = 10^{-3} \sum BB_j \times EF_{i,j}, \tag{2}$$

where $E_{i,j}$ is the emission of a gas type i (e.g., CO_2, CO, CH4, NO_X) from forest type j in megagrams (Mg), BB_j is the total BB for forest type j (in Mg), and $EF_{i,j}$ is the emission factor for gas type i (in g/kg). In Table 1 we present emission factors obtained from relevant literature (Akagi et al., 2011; Lu et al., 2011).

2.6. Mann-kendall trend analysis

The Mann-Kendall (MK) test is a widely utilized non-parametric method for detecting monotonic trends in time series data (Anees et al., 2025a, 2025b). To minimize the influence of interannual anomalies and improve trend detectability, all variables were aggregated into five-year intervals (e.g., 2001–2005, 2006–2010, etc.). This temporal smoothing approach is commonly applied in ecological trend studies to reveal persistent directional shifts while reducing noise from short-term variability. It also addresses missing or low-signal years in specific forest types or regions, enhancing statistical reliability for Mann–Kendall and Sen's Slope estimators. Its primary advantage is its ability to assess trends requiring the data to follow a specific distribution or being influenced by outliers or irregular patterns (Mehmood et al., 2024a, 2024b). The test compares Kendall's tau correlation coefficient and evaluates the significance of the trend using Z-statistics, offering a clear indication of whether the observed trend is statistically significant (Kabbilawsh et al., 2024). For two data points, x_i and x_j, the signum function, denoted as $sgn(x_i - x_j)$, assigns a value of $+1$, 0, or -1 depending on the direction of the difference (Agarwal et al., 2021; Le et al., 2020). The S statistics are computed by summing the results of the signum function for all pairs of data points:

$$S = \sum_{k=1}^{n-1} \sum_{j=k+1}^{n} sgn(x_i - x_j), \tag{3}$$

where n is the number of data points in the series. The variance of S, Var (S), is adjusted for ties in the dataset, and the Z statistic is calculated to determine the direction and significance of the trend. A positive Z value indicates an increasing trend, while a negative Z suggests a decreasing trend. Trends are considered statistically significant when the absolute value of Z exceeds 1.96 at the 5 % confidence level, suggesting a monotonic trend over time(Kabbilawsh et al., 2024).

Table 1
Emission factors for different biomass classes.

Biomass class	CO_2 (g/kg)	CO (g/kg)	CH4 (g/kg)	SO2 (g/kg)	NOx (g/kg)
EBF	1643	93	5.07	0.48	3.90
DBF	1637	89	3.92	0.32	0.75
Grassland	1686	63	1.94	0.32	0.90

2.7. Sen's slope estimator

The magnitude of the identified trends is quantified using the Sen's Slope estimator (Agarwal et al., 2021). This robust, non-parametric method calculates the median slope of the line through all possible pairs of data points, which provides an estimate of the rate of change in the time series(Ali et al., 2019). The slope for each pair of data points (x_j, x_i) is given by:

$$Q_i = \frac{x_j - x_i}{j - i}, \tag{4}$$

where x_j and x_i are the values of the time series at times j and i, respectively. The Sen's slope is then obtained by calculating the median of these pairwise slopes. If the number of data points, N, is odd, the median is simply the middle value, denoted as Q_{med}, while for even N, the median is the average of the two middle values. The confidence interval for Sen's slope is computed using the variance of S and the standard normal distribution value at the desired significance level (Agarwal et al., 2021; Deng et al., 2022; Hill and Guerschman, 2020):

$$C_{\alpha} = Z_{1-\frac{\alpha}{2}} \sqrt{Var\ (S)} \tag{5}$$

In this study, a 95 % confidence level was used to calculate the confidence bounds of Sen's Slope. However, only statistically significant slopes ($p < 0.05$) are reported in the main results. Confidence intervals are available in table S3 for reference.

These methods are particularly useful for data with irregularities or outliers, which are common in environmental studies. In this study, the MK test and Sen's Slope estimator were applied to examine the spatio-temporal trends in fire count, burnt area, and NPP across different forest types EBF, DBF, and Grassland and seasons (Dry, Wet, and Hot) from 2001 to 2023 (Bar et al., 2021; Martínez et al., 2022). By using these methods, we were able to assess both the direction and magnitude of the trends, providing insights into how fire dynamics and NPP have evolved across different vegetation types and seasonal conditions.

2.8. Kernel Density Estimation (KDE)

KDE was applied in software (version 4.4.2) using the *spatstat* package to analyze the spatial distribution of forest fires across three forest types: EBF, DBF, and grassland. Fire point data and burned area records from 2001 to 2023 were used to create continuous fire density surfaces, helping identify spatial clustering and areas with higher fire activity (Kuter et al., 2011a, 2011b). This method facilitated a better understanding of fire trends within different forest types. KDE is a non-parametric technique that estimates fire density by applying smoothing functions without assuming a specific data distribution(Buffington et al., 2021; Kuter et al., 2011b). The density at each grid cell is determined by the influence of nearby fire points, with closer points having a greater impact(Z. Zhang et al., 2017). The general equation for KDE is:

$$\widehat{f}(x) = \frac{1}{nh^d} \sum_{i=1}^{n} K\left(\frac{x - X_i}{h}\right) \tag{6}$$

where n is the number of observation points, h is the bandwidth, K is the kernel function, x is the location where the density is estimated, and X_i are the coordinates of each fire observation point. The bandwidth h controls the maximum distance over which points influence each other, under Tobler's First Law of Geography, which suggests that closer events are more related than those further apart(Shuo et al., 2021).

2.9. Machine learning models

The CO_2 emissions in this study serve as the dependent variable in the models, representing the amount of CO_2 released during forest fire events. Emission estimates for CO_2, CO, CH_4, SO_2, and NOx were calculated using established emission factors (Akagi et al., 2011; Lu et al., 2011), stratified by forest type and season (Table S2). Due to the significantly higher emission factors for CO_2 relative to other gases, its contribution was consistently the largest across all forest types and seasons, particularly during the Dry period. Thus, the analysis focused on CO_2 to capture the primary carbon fluxes associated with biomass combustion in Thailand's ecosystems. Because of its substantial impact and higher levels, CO_2 emissions were selected as the primary dependent variable for the ML models. This choice is based on the understanding that CO_2, being the most abundant emission, directly correlates with fire intensity and the scale of fire-affected areas. To better understand the relationships between the variables, Spearman rank correlation was applied to assess the strength and direction of monotonic relationships between the independent variables and CO_2 emissions(Shao et al., 2023). Additionally, multicollinearity among predictor variables was evaluated by calculating variance inflation factors (VIF) and tolerance values. The results indicated that all VIF values were less than 10, and the tolerance values were greater than 0.1, suggesting that multi-collinearity was not a concern for the model(Shahzad et al., 2024). These results, along with correlation coefficients, are presented in the supplementary materials (Figs. S1 and Table S1). By focusing on CO_2 emissions, the study seeks to understand how various environmental, topographical, and socio-economic factors such as vegetation health, land surface temperature (LST), wind speed and direction, precipitation, and human activity influence the occurrence, intensity, and spread of forest fires. For model development, the data was split into 70 % for training and 30 % for testing, ensuring an effective and unbiased evaluation of the model's predictive accuracy(Anees et al., 2024).

2.10. Random forest regression for CO_2 emission prediction

RF regression was employed to predict CO_2 emissions based on various environmental and economic factors. The RF algorithm operates by constructing an ensemble of decision trees, each built from a bootstrap sample of the training data (Ghiasi and Zendehboudi, 2021). The prediction for the target variable (CO_2 emissions) is obtained by averaging the outputs of all the individual trees in the forest. Mathematically, the predicted value Y for a given input X is computed as the means of the predictions from all the trees (Ahmad et al., 2017):

$$Y(X) = \frac{1}{B} \sum_{b=1}^{B} T_b(X) \tag{7}$$

where $Y(X)$ is the predicted CO_2 emission value for the input features X. B represents the total number of trees in the forest. $T_b(X)$ is the prediction made by the b-th tree.

For hyperparameter tuning, we used a grid search approach, which systematically explores different combinations of key parameters, such as (*n_estimators*) the number of trees in the forest, and (*max_depth*) the maximum depth of each decision tree, and (*min_samples_split)* the minimum number of samples required to split a node. This grid search ensures that the RF model achieves an optimal balance between bias and variance, which is critical for making accurate predictions without overfitting the data (Guo et al., 2016; Shao et al., 2023).

3. eXtreme gradient boosting regression for CO_2 emission prediction

In addition to RF, XGBoost was also used to predict CO_2 emissions. XGBoost is an advanced implementation of gradient boosting, an ensemble method where trees are built sequentially (T. Chen and Guestrin, 2016). Each tree in the ensemble is constructed to correct the residual errors of the previous tree, enhancing the overall model's predictive accuracy (Erdal and Karakurt, 2013; Al-Tameemi et al., 2025). XGBoost has proven to be effective in handling large datasets and improving model stability, especially when regularization is incorporated to prevent overfitting(Shahani et al., 2021). For CO_2 emissions prediction, the output $\widehat{y}_i$ for each instance i is obtained by summing the outputs of all trees in the ensemble. The prediction is expressed as follows:

$$\widehat{y}_i = \sum_{k=1}^{k} f_k(x_i)\ Where\ f_k(x_i) \in F \tag{8}$$

where x_i represents the feature values for the i-th instance. $f_k(x_i)$ is the output of the k-th regression tree. F is the set of all regression trees.

The XGBoost model was fine-tuned by adjusting key hyper-parameters; the number of boosting iterations (*nrounds*) was set to 50. This parameter determines the number of trees added to the ensemble, balancing model complexity and accuracy. (*max_depth*) Set to 8, this parameter controls the maximum depth of each tree. Deeper trees capture more complex patterns but may lead to overfitting. (*learning rate* (eta)) Set to 0.15, it controls how much each tree influences the final prediction. (*gamma*) Set to 2, it regulates tree pruning, determining the minimum loss reduction required to make a new split. (*subsample* and *colsample_bytree*) Both set to 0.8, they introduce randomness into the row and column sampling process, reducing the risk of overfitting. (*lambda (l2 regularization)* and (*alpha (l1 regularization)*) Set to 1 and 0.1, respectively, they penalize large weights, ensuring model stability and reducing the influence of noisy features. (*min_child_weight*) Set to 2, it determines the minimum number of data points required to make a split in a tree, which helps prevent overfitting(Anees et al., 2025a, 2025b). The grid search method was used to systematically evaluate combinations of these hyperparameters, ensuring that the XGBoost model was optimized for the best performance on the CO_2 emissions prediction task, and the variable's importance of RF and XGBoost are shown in Fig. S2.

3.1. Model evaluation and comparison

The performance of RF and XGBoost was evaluated using four key regression metrics: RMSE, MSE, MAE, and R^2 (Joharestani et al., 2019). RMSE provides an understanding of the average magnitude of the prediction errors by measuring the square root of the average squared differences between predicted and actual values, making it interpretable in the same units as the target variable(Chicco et al., 2021). MSE, which is like RMSE, penalizes larger errors more heavily by squaring the differences, helping to highlight outliers or large prediction discrepancies (Kumar et al., 2023). MAE, in contrast, computes the average of the absolute errors, offering a more straightforward measure of the average magnitude of the errors without amplifying large deviations(Mushtaq et al., 2024). Lastly, R^2 was used to measure the proportion of variance in the target variable that is explained by the model, with higher values indicating better explanatory power(Chai and Draxler, 2014; Chicco et al., 2021; Hosamo and Mazzetto, 2024). By evaluating both models with these metrics, the relative performance of RF and XGBoost could be determined, providing a comprehensive comparison of their predictive accuracy and suitability for the task of CO_2 emissions prediction. Beyond numerical metrics (R^2, RMSE, MAE), we provide diagnostic plots: parity plots on the independent test set, residual structure and distribution checks, and calibration curves by prediction deciles with 95 % CIs. These graphics assess agreement, error structure, calibration, and spatial transferability.

3.2. Shapley Additive Explanations (SHAP)

SHAP (Shapley Additive Explanations), derived from cooperative game theory, was employed to quantify the contribution of each input variable to the model's CO_2 emission predictions. Each feature is treated as a "player" in a game where the collective goal is accurate prediction, and its importance is evaluated by the marginal effect it has when included in or excluded from the model (Iban and Aksu, 2024; Nohara et al., 2022; Ponce-Bobadilla et al., 2024). The approach offers consistency and fairness by averaging contributions over all possible combinations of features. The contribution of a given predictor j is mathematically expressed as:

$$\varphi_j = \sum_{S\subseteq N\setminus\{j\}} \frac{|S|!(|N|-|S|-1)!}{|N|!}[f(S\cup\{J\})-F(S)] \tag{9}$$

where φ is the Shapley value for feature j, N is the full set of features, S is a subset excluding j, and $f(\cdot)$ is the model prediction function (Cakiroglu et al., 2024; Kim et al., 2024). The factorial terms provide the appropriate weighting to ensure fair attribution across all feature permutations. Unlike traditional importance measures such as gain or split count, SHAP allows both global and local interpretation of model behavior (Yu et al., 2024). Global SHAP values reflect the average absolute contribution of each feature across all predictions, while local SHAP values provide observation-specific insights into prediction drivers (Kolzow et al., 2021). This method was well-suited for evaluating emission dynamics from forest fires in Thailand, given the complexity of interactions among meteorological, topographic, and anthropogenic predictors. SHAP helped identify dominant drivers such as wind dynamics, solar radiation, and population density, allowing interpretation not only of statistical relevance but also of ecological and managerial significance (Baptista et al., 2022; UU Republik Indonesia et al., 2022).

4. Results

4.1. Spatiotemporal trends in forest fires and burnt areas across different forest types and seasons

Forest fire dynamics can be evaluated using multiple metrics, each capturing a distinct facet of fire behavior. Fire count, used here as a measure of ignition frequency, reflects the number of discrete fire events and is influenced by both natural drivers (e.g., lightning) and anthropogenic activities (e.g., slash-and-burn agriculture). However, it does not directly indicate fire severity. To provide a more comprehensive view, we analyze burnt area alongside fire count (Section 3.1) and later incorporate CO_2 emissions as a direct proxy for fire severity (Sections 3.2 and 3.3) through both empirical estimation and predictive modeling. Significant negative trends in fire count ($\tau = -0.75$, $p = 0.05$) and burnt area ($\tau = -0.94$, $p = 0.005$) were observed for EBF during the Dry season, indicating a consistent decline in fire activity (Fig. 4). The rate of decrease in fire count was estimated at −1860.94, and for burnt area at −72,869.46 ha per year. In contrast, no significant trends were detected in the Wet and Hot seasons. For DBF, trends were weak and statistically insignificant across all seasons. The Dry season showed slight declines in fire count ($\tau = -0.21$, $p = 0.43$) and burnt area ($\tau = -0.55$, $p = 0.15$), with similarly negligible trends in the Wet and Hot seasons. Grasslands displayed a moderately negative but non-significant trend in fire count during the Dry season ($\tau = -0.66$, $p = 0.09$). However, a strong and statistically significant decline in burnt area was found ($\tau = -0.99$, $p = 0.0003$), with a rate of −20,181.98 ha per year. No significant trends were noted in the Wet or Hot seasons. These results underscore the role of seasonality and vegetation type in driving fire patterns, with the Dry season exhibiting the most pronounced decline in both fire frequency and extent, particularly in EBF and Grassland ecosystems, whereas DBF remained relatively stable.

4.1.1. Sensitivity of fire counts to MODIS confidence thresholds

Evaluating fire point data at three confidence thresholds allowed us to test the strength of fire trend analysis to detection confidence.: >10 %, >30 %, and > 50 %. As expected, absolute fire counts declined with increasing confidence level; however, the interannual trajectories and seasonal peaks remained consistent across all thresholds (Fig. 5). Notably, the >10 % threshold captures lower-intensity or early-season fires that are often underrepresented at higher thresholds, particularly in DBF and grassland ecosystems. This supports its inclusion for a more comprehensive detection of fire activity in Thailand's heterogeneous tropical landscapes. The observed alignment in temporal patterns across thresholds affirms that the study's key findings are not artifacts of threshold selection, thereby reinforcing the validity of our methodological approach.

4.2. Seasonal trends in fire count and NPP across vegetation types

The relationship between fire count and NPP across three seasons (Dry, Wet, and Hot) was analyzed for different vegetation types using the MK trend test and Sen's Slope estimator, which are well-suited for detecting monotonic trends in environmental data without assuming linearity as shown in (Fig. 6). For EBF, the results revealed weak, statistically insignificant relationships across all seasons. In the Dry season, there was a minor negative trend in NPP with fire count (tau = −0.162, $p = 0.29$), though the decline was not significant. In the Wet and Hot

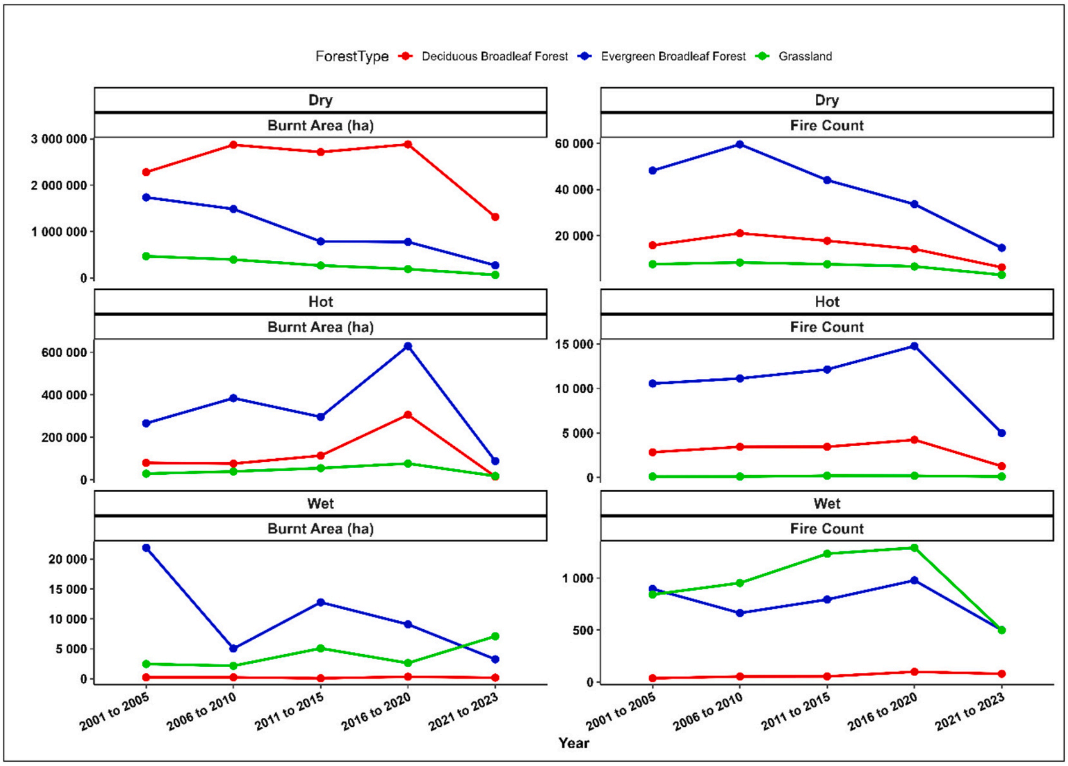

Fig. 4. Seasonal trends of burnt area (left panels) and fire count (right panels) across Thailand from 2001 to 2023, stratified by forest type [EBF (blue), DBF (red), Grassland (green)] and season [Dry, Hot, Wet]. Data is aggregated into five-year intervals to address missing or sparse seasonal detections in certain years and regions. This approach enhances statistical robustness and allows clearer identification of long-term seasonal fire patterns. (For interpretation of the references to colour in this figure legend, the reader is referred to the web version of this article.)

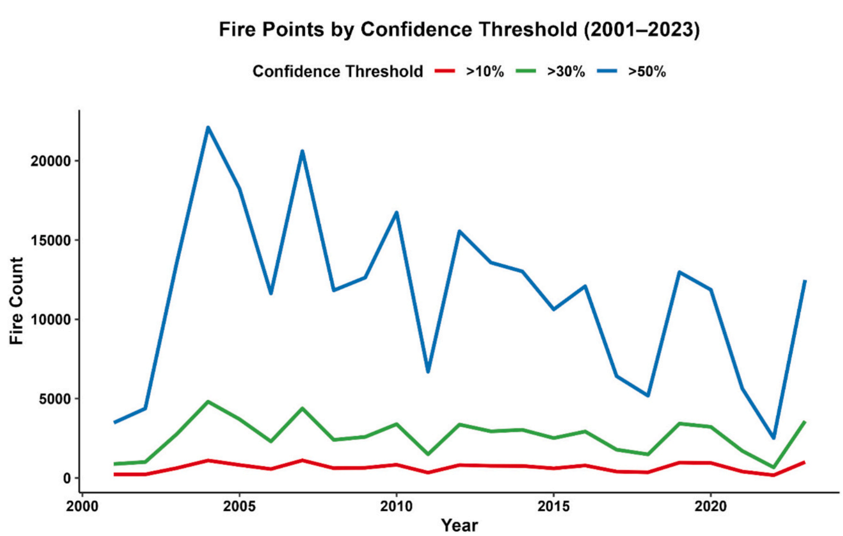

Fig. 5. Annual fire point counts across MODIS confidence thresholds (>10 %, >30 %, and > 50 %) for Thailand during 2001–2023. While absolute counts vary across thresholds, the interannual patterns are consistent, with higher-confidence detections (blue line) capturing a smaller subset of more intense fires. Lower thresholds, especially > 10 % (red line), are more inclusive and capture low-intensity and early-season fires typical of deciduous broadleaf forests and grasslands. This consistency supports the robustness of the main analysis conducted at > 10 % confidence. *(For interpretation of the references to colour in this figure legend, the reader is referred to the web version of this article.)*

seasons, weak positive relationships were observed (tau = 0.123 and 0.146, respectively), but these trends also lacked statistical significance. For DBF, a significant positive relationship was found only in the Wet season (tau = 0.69, p = 0.0007), where increasing fire counts were associated with higher NPP. The Sen's Slope of 0.98 confirmed this trend, with a clear increase in NPP as fire count rose. However, in both the Dry and Hot seasons, the relationship was weak and insignificant, with minimal changes in NPP despite fluctuations in fire count. Grasslands showed a significant positive correlation in the Hot season (tau = 0.41, p = 0.0008), indicating that higher fire counts were linked to increased NPP. The Sen's Slope of 1.21 further supported this finding, suggesting a clear rise in NPP with increasing fire count. In contrast, the Dry and Wet seasons exhibited weak or no significant relationships between fire count and NPP. Overall, the analysis highlights that fire

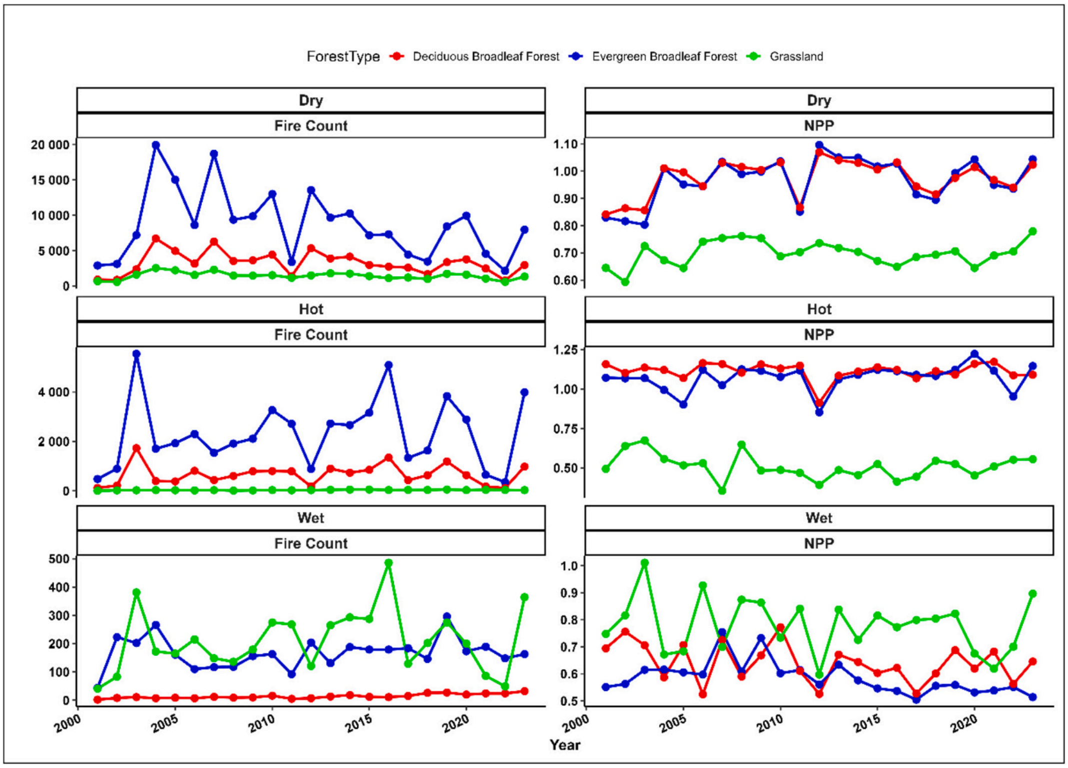

Fig. 6. Seasonal trends in fire count (left panels) and Net Primary Productivity (NPP, right panels in kg C/m^2/year) for three forest types EBF (blue), DBF (red), and Grassland (green) from 2001 to 2023. Data are shown separately for the Dry, Hot, and Wet seasons to assess fire-productivity interactions. Results illustrate differing vegetation responses, with positive NPP-fire relationships in the Hot season for Grassland and in the Wet season for DBF. (For interpretation of the references to colour in this figure legend, the reader is referred to the web version of this article.)

impacts NPP differently depending on vegetation type and season, with Grassland showing the strongest positive correlation in the Hot season, DBF exhibiting a significant relationship in the Wet season, and EBF showing weak, insignificant trends throughout all seasons.

4.3. Kernel Density Estimation (KDE) analysis

The KDE analysis revealed significant variations in the spatial distribution of fire occurrences across the study area, effectively identifying regions with differing fire densities (Fig. 7). The results showed that

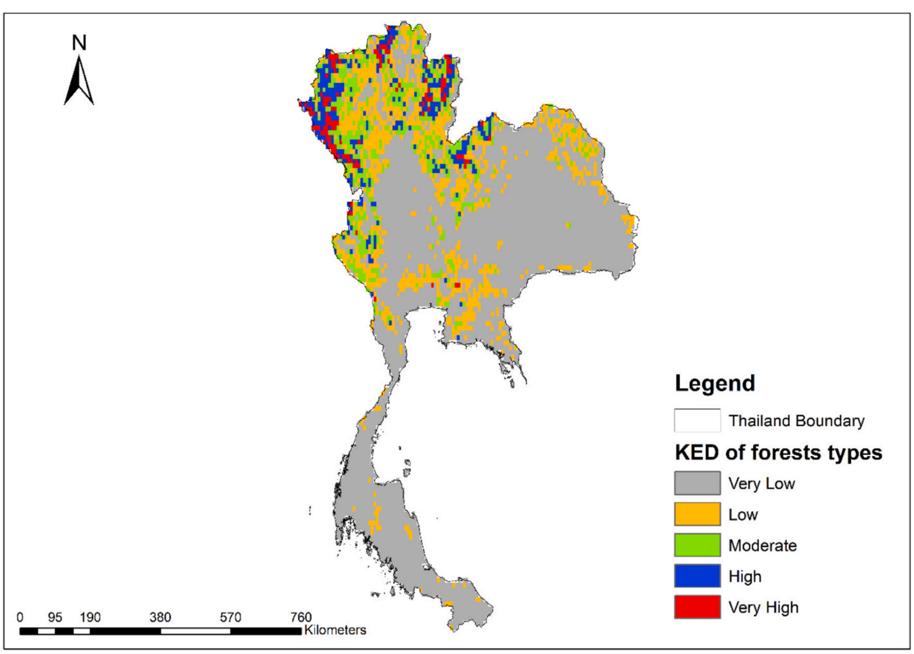

Fig. 7. Spatial distribution of forest fire intensity in Thailand based on Kernel Density Estimation (KDE) of fire event occurrences from 2001 to 2023. Density levels are classified into Very Low to Very High categories, indicating persistent hotspots in Northern and Northeastern Thailand. Map includes scale bar and north arrow for geographic reference.

Very High-Density areas, covering 2.88 % of the total area (11,887.09 km^2), represent hotspots of fire activity where clustering of fire events is most pronounced. These areas are critical for targeted fire management due to their elevated risk and potential for ecosystem degradation. In contrast, Very Low-Density areas, encompassing 56.73 % of the total area (234,170.01 km^2), exhibited minimal fire activity, likely influenced by environmental conditions or effective fire prevention measures. The spatial clustering observed aligns with Tobler's First Law of Geography, where nearby fire events exert stronger influences on density calculations, reflecting shared environmental or anthropogenic factors such as vegetation, climate, topography, or human activities. These density surfaces provide a comprehensive understanding of fire dynamics, identifying transitional zones of moderate density (11.77 %) that may signal emerging fire risks. The KDE results underscore the importance of spatially informed fire management strategies, emphasizing resource allocation in high-risk areas while maintaining monitoring efforts in regions with lower fire density. This analysis highlights KDE's robustness as a non-parametric tool for understanding spatial patterns of fire activity and provides critical insights for fire prevention, risk reduction, and sustainable land management planning.

4.4. *Estimation of seasonal emissions from forest fires across different forest types*

The emissions data for carbon-containing gases (CO_2, CO, CH4, SO_2, and NOx) across different forest types (EBF, DBF, and GRASS) from 2001 to 2023. demonstrate distinct seasonal variations (Table S2). The Dry season consistently contributed to the largest share of emissions across all forest types. The total emissions during the study period were primarily dominated by CO_2, followed by CO and CH4, with SO_2 and NOx contributing the least. Moreover, the Dry season was the largest contributor to emissions across all atmospheric components in EBF, DBF, and GRASS forests (Table 2). In EBF forests, CO_2 emissions during the Dry season accounted for 85.8 % of total seasonal emissions in 2001–2005, gradually decreasing to 74.9 % by 2021–2023. In contrast, the Hot season's share of CO_2 emissions increased from 13.1 % to 24.2 % over the same period, indicating a notable shift in seasonal fire patterns. Estimates of BB emissions were accompanied by 95 % confidence intervals, derived from replicate simulations stratified by forest type, fire season, and time. These intervals represent the range within which true emission values are likely to fall, providing a statistical measure of reliability for each estimate. For example, EBF during the dry season of 2001–2005 exhibited mean CO_2 emissions of approximately 12.24 million tons, with a 95 % confidence interval ranging from 8.39 to 16.08 million tons Table S3. In contrast, emissions for the same forest and season in 2021–2023 declined to 10.77 million tons [CI: 6.04–15.51 million], suggesting a downward trend albeit with overlapping uncertainty bounds. Wider intervals observed in Wet Forest categories and certain Grassland zones indicate higher variability, likely due to episodic fire events and lower burn consistency in these ecosystems. Such uncertainty metrics enhance the interpretive depth of emission dynamics and support more cautious inference regarding temporal changes and forest-type sensitivity.

The Wet season, in contrast, consistently contributed less than 1 % to CO_2 emissions across all periods. In DBF forests, the Dry season was even more dominant, contributing more than 90 % to CO_2 emissions across all periods, with the Hot season contribution being negligible at only 3.4 % in 2001–2005 and remaining consistently low thereafter. The Wet season had an almost negligible effect on CO_2 emissions throughout the study period. Similarly, GRASS forests exhibited a high contribution from the Dry season, with emissions in this season making up 93.7 % of CO_2 emissions in 2001–2005, and this contribution decreased slightly to 83.4 % in 2021–2023. In contrast, the Hot season contribution increased significantly, particularly from 6.0 % in 2001–2005 to 24.0 % in 2021–2023.

For other emissions, such as CO, CH4, SO_2, and NOx, the Dry season also showed the highest contribution across all forest types. The Hot season's share of emissions increased over time in both EBF and GRASS forests, particularly for CO and CH4, while the Wet season remained the smallest contributor. In EBF forests, CO emissions from the Dry season ranged from 81.9 % in 2001–2005 to 77.8 % in 2021–2023, with a slight increase in the Hot season contribution from 17.3 % to 21.6 % over the same period. For CH4 emissions, EBF forests showed a significant shift, with the Dry season contributing 79.3 % in 2001–2005, decreasing to 66.5 % by 2021–2023, while the Hot season contribution increased from 18.5 % to 31.9 % during the same period. The Wet season consistently remained a small contributor, accounting for no more than 3 % of CH4 emissions across all periods. The SO_2 and NOx emissions in EBF forests showed similar trends, with the Dry season contributing the highest percentage, peaking at 89.7 % for SO_2 in 2001–2005 and 73.9 % for NOx in the same period. The contribution of the Hot season showed a noticeable increase, especially for NOx, rising from 19.7 % in

Table 2
Seasonal temporal trends in CO_2 emissions by ecosystem type.

Years	Dry (CO_2)	Hot (CO_2)	Wet (CO_2)	Total CO_2	% Dry CO_2	% Hot CO_2	% Wet CO_2
1) Evergreen Broadleaf Forest							
2001–2005	13,580,122.03	2,082,083.54	170,207.61	15,832,413.18	85.80 %	13.10 %	1.10 %
2006–2010	11,618,755.86	3,008,424.39	39,204.03	14,666,384.29	79.20 %	20.50 %	0.30 %
2011–2015	6,156,585.90	2,310,126.80	99,562.70	8,566,275.40	71.80 %	27.00 %	1.20 %
2016–2020	6,089,434.47	4,922,047.03	71,033.05	11,082,514.54	55.00 %	44.40 %	0.60 %
2021–2023	2,135,455.36	687,817.31	25,230.32	2,848,503.99	74.90 %	24.20 %	0.90 %
2) Deciduous Broadleaf Forest							
Years	**Dry (CO_2)**	**Hot (CO_2)**	**Wet (CO_2)**	**Total CO_2**	**% Dry CO_2**	**% Hot CO_2**	**% Wet CO_2**
2001–2005	18,736,078.88	652,549.13	1841.63	19,390,469.63	96.60 %	3.40 %	0.01 %
2006–2010	23,585,077.50	626,152.50	1841.63	24,213,071.63	97.40 %	2.60 %	0.01 %
2011–2015	22,306,989.75	930,634.50	613.875	23,238,238.13	95.90 %	4.00 %	0.00 %
2016–2020	23,651,171.38	2,512,590.38	2660.13	26,166,421.88	90.30 %	9.60 %	0.01 %
2021–2023	10,801,130.63	121,956.50	1432.38	10,924,519.51	99.90 %	1.10 %	0.01 %
3) Grassland							
Years	**Dry (CO_2)**	**Hot (CO_2)**	**Wet (CO_2)**	**Total CO_2**	**% Dry CO_2**	**% Hot CO_2**	**% Wet CO_2**
2001–2005	947,305.44	58,412.00	4955.26	1,010,672.70	93.70 %	5.80 %	0.50 %
2006–2010	803,302.60	78,833.67	4354.62	886,490.90	90.60 %	8.90 %	0.50 %
2011–2015	545,579.06	110,317.09	10,160.78	665,057.93	82.00 %	16.60 %	1.50 %
2016–2020	392,766.87	156,015.59	5305.63	554,087.09	70.80 %	28.20 %	1.00 %
2021–2023	135,593.92	34,887.03	14,215.09	184,696.03	73.50 %	18.90 %	7.70 %

2001–2005 to 28.0 % in 2021–2023. The Wet season contributions for both SO_2 and NOx remained minor, typically under 5 %. In GRASS ecosystems, the Dry season was the most significant contributor to CO_2, CO, and CH4 emissions, but the Hot season contribution steadily increased over the years, particularly for CO and CH4. For SO_2 and NOx, the Dry season remained the dominant contributor, although there was a slight increase in the Hot season contribution, particularly in the later periods of the study. In all forest types, CO_2 emissions were predominantly generated in the Dry season, with the Hot season gradually contributing more to emissions over time. The Wet season consistently exhibited the smallest share of emissions across all gases, confirming its limited role in the overall carbon emissions from forest fires. The seasonal variations observed may be attributed to changes in environmental conditions, including temperature and precipitation, which influence the intensity and frequency of forest fires.

4.5. Evaluation of RF and XGBoost model performance for CO_2 emissions prediction

4.5.1. Model performance metrics

The predictive capability of RF and XGBoost models for estimating CO_2 emissions from forest fires in Thailand was evaluated using four standard regression metrics: RMSE, Mean Square Error (MSE), Mean Absolute Error (MAE), and the coefficient of determination (R^2) (Table 3). On the training dataset, both models demonstrated strong performance, with RMSE values of 261.61 (RF) and 261.40 (XGBoost), and R^2 values of 0.9524 and 0.9525, respectively. This indicates high model accuracy and a strong fit to the training data. However, model performance decreased when applied to the test dataset. The RF model yielded an RMSE of 550.79 and an R^2 of 0.7919, while XGBoost produced an RMSE of 559.09 and an R^2 of 0.7856. MAE values also more than doubled on the test set, from 196.11 (RF) and 194.84 (XGBoost) during training to 419.78 and 422.75, respectively, on testing. This reduction in predictive accuracy reflects a degree of overfitting in both models, where training performance was not fully generalizable to unseen data. Nevertheless, R^2 values above 0.78 on the test set indicate that both models still explain a substantial proportion of the variability in CO_2 emissions and thus offer useful insights into fire-emission relationships. Visual diagnostics corroborate these metrics. Parity plots indicate close adherence to the 1:1 line with fitted slopes near unity for both RF and XGBoost) on the independent test set (Fig. S4). Residuals show no pronounced heteroscedasticity, and Q–Q plots display only modest tail departures (Fig. S5). Calibration curves align with the identity line across prediction deciles, with limited deviation in the upper deciles (Fig. S6).

4.5.2. Spatial prediction and regional variation

CO_2 emissions were spatially predicted across Thailand using both models (Fig. 8). The resulting emission maps revealed significant regional variation, highlighting provinces with higher estimated fire-related emissions. In Central Thailand, provinces such as Kanchanaburi, Ratchaburi, Phetchaburi, Prachuap Khiri Khan, Sa Kaeo, and Prachin Buri consistently exhibited moderate to high predicted emissions. This suggests that forest fires in these areas are potentially linked to land use change, regional climatic variations, or anthropogenic burning. In Northeastern Thailand, provinces including Chaiyaphum, Loei, Khon Kaen, Nakhon Ratchasima, Buri Ram, and Maha Sarakham showed elevated CO_2 emissions. The region's agricultural activities and seasonal fire practices likely contributed to these outcomes. Northern Thailand, with its mountainous terrain and prolonged dry season, demonstrated the highest emission intensities, particularly in provinces such as Mae Hong Son, Chiang Mai, Lampang, Lamphun, and Chiang Rai. Conversely, Southern Thailand exhibited comparatively lower emission levels. Provinces such as Ranong, Surat Thani, Yala, and Narathiwat displayed only moderate fire-induced emissions, which may be attributed to the region's humid tropical climate and limited seasonal burning. These spatial disparities emphasize the necessity of regionally tailored fire mitigation strategies, informed by emission intensity and landscape context.

Table 3
Performance metrics for RF and XGBoost models on training and testing data.

Metric	RF_Train	RF_Test	XGBoost_Train	XGBoost_Test
RMSE	261.61	550.79	261.40	559.09
MSE	68,438	303,375	68,329.12	312,581.20
MAE	196.11	419.78	194.84	422.75
R^2	0.9524	0.7919	0.9525	0.7856

4.6. Shapley Additive Explanations (SHAP) analysis

The drivers of predicted CO_2 emissions were evaluated by magnitude and direction of feature influence using SHAP summary plots (Fig. 9). Wind dynamics particularly V Wind and U Wind emerged as the most influential variables, reflecting their critical role in modulating fire spread, combustion efficiency, and subsequent CO_2 release. Solar radiation followed closely, suggesting its importance in influencing fuel dryness and ignition potential. Population density also showed strong SHAP values, indicating that anthropogenic activities substantially contribute to fire-induced emissions. In contrast, topographic variables like slope and aspect had limited overall impact, implying that terrain plays a secondary role in determining emission levels.

The variability of driver influence was further evaluated by conducting an additional SHAP analysis using fire count as the dependent variable, holding all predictors constant. This alternative model revealed both convergences and divergences in feature importance. While wind components remained dominant in both models, elevation, aspect, and precipitation showed significantly higher SHAP values in the fire count model, particularly in upland regions (Fig. S3). This suggests that topographic and hydrological constraints exert stronger control on fire occurrence, while emission magnitude is more sensitive to energy-related and anthropogenic factors such as LST and population density. Additionally, we stratified the SHAP outputs by vegetation type (EBF, DBF, and Grassland) to capture ecosystem-specific interactions. In Grasslands, SHAP values for evaporation and LST were markedly higher, consistent with their open canopy and greater surface exposure. Conversely, in EBF, precipitation showed greater influence, likely due to its role in fuel moisture retention under dense canopies. These stratified results highlight that driver importance is not uniform, and ecological context plays a critical role in modulating fire dynamics. Overall, SHAP results provide transparent, interpretable insights into both the spatial variability and relative influence of environmental and anthropogenic drivers across fire models. These findings underscore the utility of integrating local terrain, land use, and climatic variability into region-specific fire mitigation and emission reduction strategies.

5. Discussion

The analysis of spatiotemporal trends in forest fires, burnt areas, fire count, and their relationship with seasonal dynamics and vegetation types reveals important insights into the patterns of forest fire activity across different ecosystems. These findings have significant implications for both ecological and management perspectives, particularly in the context of fire-driven emissions and the role of fire in ecosystem dynamics.

5.1. Spatiotemporal trends in forest fires and burnt areas

The spatiotemporal analysis revealed important variations in fire behavior across vegetation types and seasons. In EBF, the decline in fire count and burnt area during the Dry season suggests possible improvements in fire management or the influence of wetter climatic conditions

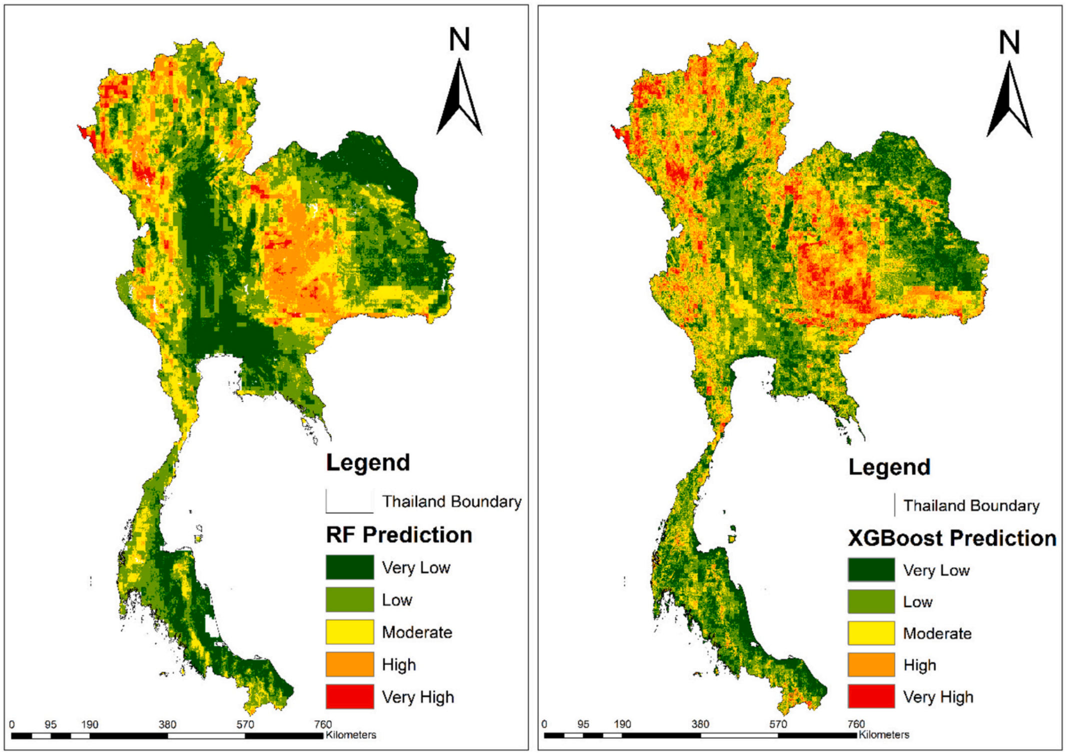

Fig. 8. Prediction CO_2 emissions in Thailand on Random Forest and XGBoost models.

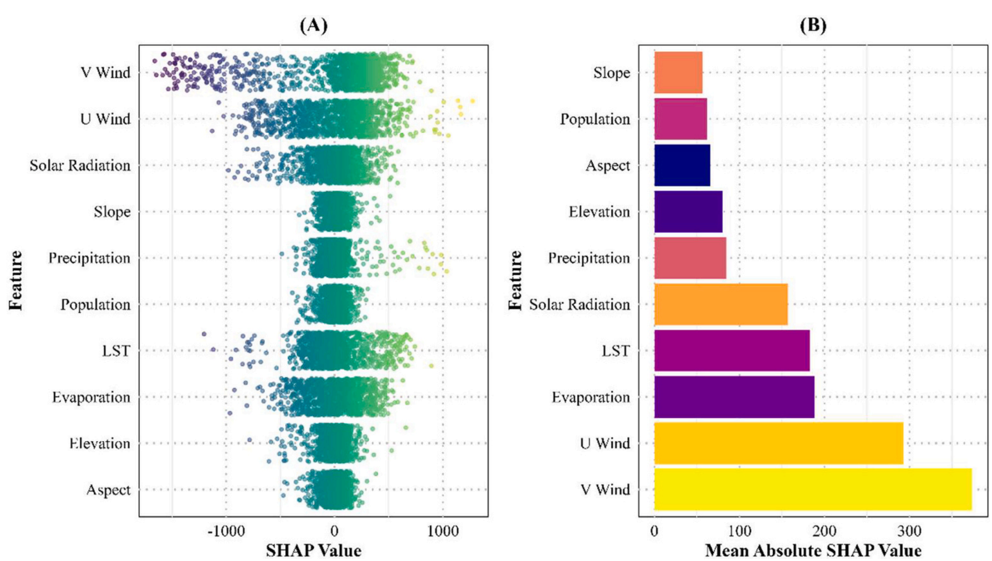

Fig. 9. SHAP-based interpretation of feature influence on CO_2 emissions.
(A) Summary plot showing individual SHAP value distributions for each predictor across the dataset. Feature values are colour-coded, with the x-axis representing the SHAP impact on model output. (B) Bar chart ranking features by their mean absolute SHAP values, reflecting overall importance in the model's emission predictions.

such as increased early-season rainfall. This aligns with Hurteau et al. (2014), who reported similar declining trends in fire-prone regions. The absence of significant trends in the Wet and Hot seasons may reflect higher precipitation levels and reduced ignition potential during these periods (Shirazi et al., 2017). In DBF, the fire trends appeared weaker, with relatively stable fire frequency across seasons. This stability may be linked to human-induced factors such as land-use change and traditional agricultural burning practices, as supported by Zhan et al. (2023). Slight increases observed during the Hot season may reflect complex interactions between vegetation dryness and reduced management enforcement. Grassland ecosystems showed a notable decline in burnt areas, even where fire count decreased only moderately. This could reflect improved surface fire control or shifts in vegetation composition limiting fire spread. While grasslands have historically experienced high fire frequency during dry conditions (Kirillina et al., 2020), these new patterns may indicate a shift in fire regime due to land-use interventions. The lack of significant changes during the Wet and Hot seasons further suggests that anthropogenic influences may now outweigh seasonal climatic factors (Littell et al., 2016; Mouillot et al., 2002). Overall, these findings highlight the influence of both seasonal dynamics and ecosystem characteristics, shaped by climatic variability and human activity, in governing Thailand's forest fire patterns.

5.2. Fire count and net primary productivity

The analysis of the relationship between fire count and NPP across seasons underscores the complexity of fire-ecosystem interactions. In EBF forests, no significant correlations were observed between fire count and NPP, indicating that fire frequency may not directly affect productivity in these ecosystems(Heisler et al., 2004; Song and Liu, 2019). This lack of correlation could be attributed to the resilience of Evergreen forests to fire, where fire events might not substantially alter long-term productivity or growth(Donato et al., 2009). On the other hand, DBF exhibited a strong positive correlation between fire count and NPP in the Wet season ($R^2 = 0.69$, $p = 0.0007$). This suggests that fire events can stimulate higher productivity in these forests, possibly by promoting the release of nutrients from burnt biomass or encouraging new growth following fire events(Carter and Foster, 2004). The Wet season's increased productivity could stem from the flushing effect of fire, where soil nutrients become more available for plant uptake after fires, facilitating enhanced vegetation growth(Kominoski et al., 2022). For Grasslands, the Hot season showed a significant positive relationship between fire count and NPP ($R^2 = 0.41$, $p = 0.0008$). Grasslands are inherently adapted ecosystems, where fire plays a critical role in maintaining vegetation dynamics(Keeley and Pausas, 2022). In this season, fire may stimulate the growth of fire-adapted species by reducing competition, promoting nutrient cycling, and increasing the availability of light and space for grasses and herbaceous plants(Adie and Lawes, 2023; Sun et al., 2023).

5.3. Emissions from forest fires

The analysis of emissions from forest fires between 2001 and 2023 reveals distinct seasonal variations across different forest types. The Dry season consistently accounted for the largest share of emissions across EBF, DBF, and Grassland ecosystems, with EBF forests showing CO_2 emissions contributing 85.8 % of total emissions during 2001–2005, which declined slightly to 74.9 % by 2021–2023. This reduction, combined with an increase in emissions during the Hot season (from 13.1 % to 24.2 %), suggests a shift in fire occurrence patterns, potentially linked to rising temperatures and altered precipitation due to climate change (Romanov et al., 2022). This aligns with studies indicating that changing climatic conditions can drive shifts in fire regimes, leading to increased intensity and frequency of fires, exacerbating carbon emissions. In DBF forests, the Dry season consistently contributed over 90 % of emissions throughout the study period, highlighting these forests' vulnerability to fire during dry months. This pattern suggests that climate change, particularly drying trends, could exacerbate fire risks and their associated emissions in these forest types (Zhao et al., 2005; Anees et al., 2025). The Wet season, by contrast, contributed less than 1 % across all forest types, underscoring its role in suppressing fire activity due to higher moisture availability. Grassland ecosystems exhibited similar trends, with the Dry season contributing 93.7 % of CO_2 emissions in the earlier years, decreasing slightly to 83.4 % by 2021–2023. This decline, coupled with a rise in emissions from the Hot season, particularly CO and CH4, suggests a changing fire regime, potentially linked to longer and more intense fire seasons driven by climate change (Podur and Wotton, 2010; Zhao et al., 2005).

Notably, CH_4 emissions during the Hot season increased from 18.5 % to 31.9 % over the study period, indicating a shift in seasonal fire activity rather than a simple intensification of the Dry season. While the Dry season historically dominated emissions particularly in DBF where it still contributes over 90 % recent trends in EBF and Grassland ecosystems show a relative decline in Dry season emissions and a rise in Hot season emissions, particularly for CO and CH_4. These changes suggest a transition in fire regime timing, potentially driven by altered precipitation patterns or extended heat periods linked to climate change (Podur and Wotton, 2010; Zhao et al., 2005; Knapp et al., 2009). This evolving seasonality underscores the need for adaptive fire management strategies that also consider the growing role of the Hot season, rather than focusing solely on traditional Dry season controls (Van Der Werf et al., 2010).

5.4. Model performance, generalization challenges, and environmental insights in CO_2 emissions prediction from forest fires

The performance of both RF and XGBoost models in predicting CO_2 emissions from forest fires in Thailand is consistent with prior studies in environmental modeling. As observed by **Granell et al. (2013)** and **Pichler and Hartig (2023)**, such models often achieve strong results on training data but face generalization difficulties when applied to unseen testing data. In this study, both models performed similarly on the training set, with RMSE values around 261. However, their performance dropped on the testing set, with RMSEs rising to 550.79 for RF and 559.09 for XGBoost. This decline reflects the broader challenge highlighted by **Campolongo and Saltelli (1997)** and **Konya and Nematzadeh (2024)**, who noted the difficulty of capturing complex, nonlinear environmental processes in generalizable models. Despite this performance drop, both models were able to explain a significant portion of the variance in CO_2 emissions, achieving R^2 values above 0.78. This suggests they retain explanatory value for understanding emission dynamics. As noted by Domingo et al. (2017), even moderately predictive models can offer ecological insight when interpreted cautiously, especially if supported by robust feature attribution methods. Spatially, high CO_2 emissions were concentrated in Central, Northeastern, and Northern Thailand, consistent with Punsompong et al. (2021) and Shi et al. (2014), who attributed fire intensity in these areas to agricultural activity and regional climate. In contrast, Southern Thailand exhibited lower emissions, which is expected given its tropical evergreen forests, higher rainfall, and limited open burning (Lebel, 2009; Taylor, 2010).

The SHAP analysis further reinforced the importance of wind dynamics, as V Wind and U Wind were among the top predictors. This aligns with the findings of Agastra (2022) and Buch et al. (2023), who also identified wind as a major factor influencing fire spread and intensity. Other influential variables, such as solar radiation and elevation, reflected nonlinear interactions previously documented in Shahzad et al. (2024) and Wang et al. (2024), highlighting the ecological complexity of emission behavior. To enhance the predictive accuracy of such models, future research should emphasize hyperparameter tuning, k-fold spatial cross-validation, and feature engineering, as recommended by Konya and Nematzadeh (2024). Exploring neural networks or other deep learning approaches may offer improved performance in capturing complex interactions. The integration of higher temporal resolution data, such as daily fire dynamics or near-real-time meteorological variables, could further strengthen model responsiveness and interpretability. Additionally, future work should focus on the role of human-induced land-use changes, especially in DBF regions where anthropogenic burning remains prevalent. Lastly, expanding the SHAP analysis to explore interaction effects can help uncover synergistic influences such as how solar radiation amplifies wind-driven fires or how topography modulates fuel load thereby informing more effective fire prevention and carbon mitigation strategies.

6. Conclusion

This study provides a spatially explicit assessment of forest fire dynamics and their emissions across Thailand's ecosystems from 2001 to 2023. Findings confirm the Dry season as the primary period of fire activity, particularly in EBF and Grassland regions, with emerging shifts toward increased emissions in the Hot season. CO_2 was identified as the dominant greenhouse gas, and predictive modeling using RF and

XGBoost successfully captured emission trends, with SHAP analysis revealing key environmental drivers such as wind dynamics and solar radiation. While the models explained substantial variance in CO_2 emissions, limitations include the reliance on global emission factors and coarse temporal resolution of fire data, which constrain finer-scale fire behavior analysis. Future research should focus on developing region-specific emission factors, integrating sub-daily fire records, and incorporating socioeconomic drivers such as land-use change and fire suppression capacity. These insights underscore the need for adaptive, region-specific fire management particularly in Northern and Northeastern Thailand and support the design of early-warning systems, REDD+ implementation, and sustainable BB policies under evolving climate and land-use pressures.

Availability of data and material

The authors confirm that the data links supporting the findings of this study are available within the article.

Acknowledgments and Funding details

FS, KM, SAA, MA, KH, WRK, PJ and MS acknowledge the support of the Precision Forestry Key Laboratory of Beijing, Beijing Forestry University and King Mongkut's Institute of Technology Ladkrabang, Prince of Chumphon Campus, Chumphon 86,160, Thailand for helping and platforms for this research. MO and JGB research are supported by FCT – Fundação para a Ciência e a Tecnologia, I.P., through the projects UID/4674/2025 of the Research Center in Mathematics and Applications and UID/00239/2025 (DOI: 10.54499/UID/00239/2025) and UID/PRR/00239/2025 (DOI: 10.54499/UID/PRR/00239/2025) of the Forest Research Centre as well as by the project ref. H2020-MSCA-RISE-2020/101007950, with the title "DecisionES - Decision Support for the Supply of Ecosystem Services under Global Change", funded by the Marie Curie International.

CRediT authorship contribution statement

Fahad Shahzad: Writing – original draft, Visualization, Validation, Software, Methodology, Investigation, Formal analysis, Data curation, Conceptualization. **Kaleem Mehmood:** Writing – review & editing, Visualization, Validation, Supervision. **Shoaib Ahmad Anees:** Writing – review & editing. **Muhammad Adnan:** Writing – review & editing. **Khadim Hussain:** Writing – review & editing. **Waseem Razzaq Khan:** Writing – review & editing. **Munawar Shah:** Writing – review & editing. **Punyawi Jamjareegulgarn:** Writing – review & editing, Validation, Investigation. **Manuela Oliveira:** Writing – review & editing, Formal analysis, Supervision. **José G. Borges:** Writing – review & editing.

Informed consent statement

Not applicable.

Consent

Informed consent was obtained from all participants involved in this study. Participants were provided with detailed information about the research objectives, procedures, potential risks, and benefits before agreeing to participate. They were assured that their participation was voluntary, and they had the right to withdraw from the study at any time without facing any consequences.

All participants were informed about the confidentiality measures in place to protect their identity and personal information. Data collected during the study will be used solely for research purposes and will be securely stored.

This study was conducted in accordance with ethical standards and guidelines, and participants were encouraged to ask questions and seek clarification at any stage of the research process. If you have any further questions or concerns regarding the consent process, please contact fahadshahzadbjfu@gmail.com.

Ethical approval

This research did not involve human or animal subjects; therefore, formal ethical approval was not required. The study strictly adheres to general ethical principles, and the authors are committed to upholding the highest standards of ethical research conduct. Any potential conflicts of interest that could have influenced the ethical conduct of this research have been declared.

Institutional review board statement

Not applicable.

Declaration of competing interest

The authors declare no conflicts of interest that could have influenced the ethical conduct of this research.

Appendix A. Supplementary data

Supplementary data to this article can be found online at https://doi.org/10.1016/j.gloplacha.2025.105236.

Data availability

Data will be made available on request.

References

Abatzoglou, J.T., Dobrowski, S.Z., Parks, S.A., Hegewisch, K.C., 2018. TerraClimate, a high-resolution global dataset of monthly climate and climatic water balance from 1958–2015. Scientific data 5 (1), 1–12.
Adam, M.G., Tran, P.T.M., Bolan, N., Balasubramanian, R., 2021. Biomass burning-derived airborne particulate matter in Southeast Asia: A critical review. J. Hazard. Mater. 407. https://doi.org/10.1016/j.jhazmat.2020.124760.
Adie, H., Lawes, M.J., 2023. Solutions to fire and shade: resprouting, growing tall and the origin of Eurasian temperate broadleaved forest. Biol. Rev. 98 (2). https://doi.org/10.1111/brv.12923.
Agarwal, S., Suchithra, A.S., Singh, S.P., 2021. Analysis and interpretation of rainfall trend using Mann-Kendall's and Sen's slope Method. Indian J. Ecol. 48 (2).
Agastra, A., 2022. Forecasting Prescribed Fires Using Weather Forecasts, Satellite Data, and Machine Learning. The Florida State University.
Ahmad, M.W., Mourshed, M., Rezgui, Y., 2017. Trees vs Neurons: Comparison between random forest and ANN for high-resolution prediction of building energy consumption. Energ. Buildings 147. https://doi.org/10.1016/j.enbuild.2017.04.038.
Akagi, S.K., Yokelson, R.J., Wiedinmyer, C., Alvarado, M.J., Reid, J.S., Karl, T., Crounse, J.D., Wennberg, P.O., 2011. Emission factors for open and domestic biomass burning for use in atmospheric models. Atmos. Chem. Phys. 11 (9). https://doi.org/10.5194/acp-11-4039-2011.
Alaganthiran, J.R., Chenayah, S., Rasiah, R., 2025. What are the Current Determinants that Influence the Total Amount of Greenhouse gases Produced by selected Asian Nations? Institut. Econ. 111–137.
Ali, R., Kuriqi, A., Abubaker, S., Kisi, O., 2019. Long-term trends and seasonality detection of the observed flow in Yangtze River using Mann-Kendall and Sen's innovative trend method. Water (Switzerland) 11 (9). https://doi.org/10.3390/w11091855.
Al-Tameemi, N., Zhang, X., Shahzad, F., Mehmood, K., Xiao, L., Zhou, J., 2025. From trends to drivers: Vegetation degradation and land-use change in Babil and Al-Qadisiyah, Iraq (2000–2023). Remote Sens. 17 (19). https://doi.org/10.3390/rs17193343. Article 3343.
Aman, N., Panyametheekul, S., Pawarmart, I., Sudhibrabha, S., Manomaiphiboon, K., 2025. A Visibility-based Historical PM2. 5 Estimation for four decades (1981–2022) using Machine Learning in Thailand: Trends, Meteorological Normalization, and Influencing Factors using SHAP Analysis. Aerosol Air Qual. Res. 25 (1), 1–17.
Anees, S.A., Mehmood, K., Rehman, A., Rehman, N.U., Muhammad, S., Shahzad, F., Hussain, K., Luo, M., Alarfaj, A.A., Alharbi, S.A., Khan, W.R., 2024. Unveiling fractional vegetation cover dynamics: A spatiotemporal analysis using MODIS NDVI and machine learning. Environ. Sustain. Indic. 24 (September), 100485. https://doi.org/10.1016/j.indic.2024.100485.
Anees, S.A., Mehmood, K., Khan, W.R., Shahzad, F., Zhran, M., Ayub, R., Alarfaj, A.A., Alharbi, S.A., Liu, Q., 2025a. Spatiotemporal dynamics of vegetation cover:

integrative machine learning analysis of multispectral imagery and environmental predictors. Earth Sci. Inf. 18 (1), 1–23.
Anees, S.A., Mehmood, K., Luo, M., Abuelgasim, A., Pan, S.A., Shahzad, F., Khan, W.R., 2025b. Advancing forest fire burn severity and vegetation recovery assessments using remote sensing and machine learning approaches. Eco. Inform. 103446.
Baek, D.H., Seo, Y.B., Gil, J.S., Lee, M.H., Lee, J.S., Lee, G.W., Kim, J.C., 2025. An Investigation of Benzene, Toluene, Ethylbenzene, m, p-xylene; Biogenic Volatile Organic Compounds; and Carbonyl Compounds in Chiang Mai's Atmosphere and Estimation of their Emission sources during the Episode Period. Atmosphere 16 (3), 342.
Baptista, M.L., Goebel, K., Henriques, E.M.P., 2022. Relation between prognostics predictor evaluation metrics and local interpretability SHAP values. Artif. Intell. 306. https://doi.org/10.1016/j.artint.2022.103667.
Bar, S., Parida, B.R., Roberts, G., Pandey, A.C., Acharya, P., Dash, J., 2021. Spatio-temporal characterization of landscape fire in relation to anthropogenic activity and climatic variability over the Western Himalaya, India. GISci. Rem. Sens. 58 (2). https://doi.org/10.1080/15481603.2021.1879495.
Bentéjac, C., Csörgő, A., Martínez-Muñoz, G., 2021. A comparative analysis of gradient boosting algorithms. Artif. Intell. Rev. 54 (3). https://doi.org/10.1007/s10462-020-09896-5.
Beringer, J., Hutley, L.B., Abramson, D., Arndt, S.K., Briggs, P., Bristow, M., Canadell, J. G., Cernusak, L.A., Eamus, D., Edwards, A.C., Evans, B.J., Fest, B., Goergen, K., Grover, S.P., Hacker, J., Haverd, V., Kanniah, K., Livesley, S.J., Lynch, A., Uotila, P., 2015. Fire in Australian savannas: from leaf to landscape. In: *Global Change Biology* (Vol. 21, issue 1). https://doi.org/10.1111/gcb.12686.
Bessagnet, B., Allemand, N., Putaud, J.P., Couvidat, F., André, J.M., Simpson, D., Pisoni, E., Murphy, B.N., Thunis, P., 2022. Emissions of carbonaceous particulate matter and ultrafine particles from vehicles—a scientific review in a cross-cutting context of air pollution and climate change. In: *Applied Sciences (Switzerland)* (Vol. 12, issue 7). https://doi.org/10.3390/app12073623.
Bhagat, S.K., Tiyasha, T., Awadh, S.M., Tung, T.M., Jawad, A.H., Yaseen, Z.M., 2021. Prediction of sediment heavy metal at the Australian Bays using newly developed hybrid artificial intelligence models. Environ. Pollut. 268. https://doi.org/10.1016/j.envpol.2020.115663.
Bot, K., Borges, J.G., 2022. A Systematic Review of applications of Machine Learning Techniques for Wildfire Management Decision support. Inventions 7, 15. https://doi.org/10.3390/inventions7010015.
Buch, J., Williams, A.P., Juang, C.S., Hansen, W.D., Gentine, P., 2023. SMLFire1. 0: a stochastic machine learning (SML) model for wildfire activity in the western United States. Geosci. Model Dev. 16 (12), 3407–3433.
Buffington, T., Scott, J.G., Ezekoye, O.A., 2021. Combining spatial and sociodemographic regression techniques to predict residential fire counts at the census tract level. Comput. Environ. Urban. Syst. 88, 101633.
Cakiroglu, C., Demir, S., Ozdemir, M.H., Aylak, B.L., Sariisik, G., Abualigah, L., 2024. Data-driven interpretable ensemble learning methods for the prediction of wind turbine power incorporating SHAP analysis. Expert Syst. Appl. 237, 121464.
Campolongo, F., Saltelli, A., 1997. Sensitivity analysis of an environmental model: An application of different analysis methods. Reliab. Eng. Syst. Saf. 57 (1). https://doi.org/10.1016/S0951-8320(97)00021-5.
Carter, M.C., Foster, C.D., 2004. Prescribed burning and productivity in southern pine forests: A review. For. Ecol. Manag. 191 (1–3). https://doi.org/10.1016/j.foreco.2003.11.006.
Chai, T., Draxler, R.R., 2014. Root mean square error (RMSE) or mean absolute error (MAE)?–Arguments against avoiding RMSE in the literature. Geosci. Model Dev. 7 (3), 1247–1250.
Chen, T., Guestrin, C., 2016. Xgboost: A scalable tree boosting system. In: Proceedings of the 22nd Acm Sigkdd International Conference on Knowledge Discovery and Data Mining, pp. 785–794.
Chen, J., Li, C., Ristovski, Z., Milic, A., Gu, Y., Islam, M.S., Wang, S., Hao, J., Zhang, H., He, C., Guo, H., Fu, H., Miljevic, B., Morawska, L., Thai, P., LAM, Y.F., Pereira, G., Ding, A., Huang, X., Dumka, U.C., 2017. A review of biomass burning: Emissions and impacts on air quality, health and climate in China. Sci. Total Environ. 579. https://doi.org/10.1016/j.scitotenv.2016.11.025.
Chicco, D., Warrens, M.J., Jurman, G., 2021. The coefficient of determination R-squared is more informative than SMAPE, MAE, MAPE, MSE and RMSE in regression analysis evaluation. PeerJ Comput. Sci. 7. https://doi.org/10.7717/PEERJ-CS.623.
Deng, M., Meng, X., Lu, Y., Li, Z., Zhao, L., Niu, H., Chen, H., Shang, L., Wang, S., Sheng, D., 2022. The Response of Vegetation to Regional climate Change on the Tibetan Plateau based on Remote Sensing Products and the Dynamic Global Vegetation Model. Remote Sens. 14 (14). https://doi.org/10.3390/rs14143337.
deRichter, R., Caillol, S., 2011. Fighting global warming: the potential of photocatalysis against CO2, CH4, N2O, CFCs, tropospheric O3, BC and other major contributors to climate change. In. J. Photochem. Photobiol. C Photchem. Rev. 12, Issue 1. https://doi.org/10.1016/j.jphotochemrev.2011.05.002.
Domingo, D., Lamelas-Gracia, M.T., Montealegre-Gracia, A.L., de la Riva-Fernández, J., 2017. Comparison of regression models to estimate biomass losses and CO2 emissions using low-density airborne laser scanning data in a burnt Aleppo pine forest. Eur. J. Remote Sens. 50 (1). https://doi.org/10.1080/22797254.2017.1336067.
Donato, D.C., Fontaine, J.B., Robinson, W.D., Kauffman, J.B., Law, B.E., 2009. Vegetation response to a short interval between high-severity wildfires in a mixed-evergreen forest. J. Ecol. 97 (1). https://doi.org/10.1111/j.1365-2745.2008.01456.x.
Erdal, H.I., Karakurt, O., 2013. Advancing monthly streamflow prediction accuracy of CART models using ensemble learning paradigms. J. Hydrol. 477. https://doi.org/10.1016/j.jhydrol.2012.11.015.
Ghiasi, M.M., Zendehboudi, S., 2021. Application of decision tree-based ensemble learning in the classification of breast cancer. Comput. Biol. Med. 128. https://doi.org/10.1016/j.compbiomed.2020.104089.
Giglio, L., Boschetti, L., Roy, D.P., Humber, M.L., Justice, C.O., 2018. The Collection 6 MODIS burned area mapping algorithm and product. Remote Sens. Environ. 217, 72–85.
Granell, C., Díaz, L., Schade, S., Ostländer, N., Huerta, J., 2013. Enhancing integrated environmental modelling by designing resource-oriented interfaces. Environ. Model. Softw. 39. https://doi.org/10.1016/j.envsoft.2012.04.013.
Grutzen, P.J., Andreae, M.O., 1990. Biomass burning in the tropics: Impact on atmospheric chemistry and biogeochemical cycles. Science 250 (4988). https://doi.org/10.1126/science.250.4988.1669.
Guo, F., Wang, G., Su, Z., Liang, H., Wang, W., Lin, F., Liu, A., 2016. What drives forest fire in Fujian, China? Evidence from logistic regression and Random Forests. Int. J. Wildland Fire 25 (5), 505–519.
Heisler, J.L., Briggs, J.M., Knapp, A.K., Blair, J.M., Seery, A., 2004. Direct and indirect effects of fire on shrub density and aboveground productivity in a Mesic grassland. Ecology 85 (8). https://doi.org/10.1890/03-0574.
Hill, M.J., Guerschman, J.P., 2020. The MODIS global vegetation fractional cover product 2001-2018: Characteristics of vegetation fractional cover in grasslands and savanna woodlands. Remote Sens. 12 (3). https://doi.org/10.3390/rs12030406.
Hosamo, H., & Mazzetto, S. (2024). Performance Evaluation of Machine Learning Models for predicting Energy Consumption and Occupant Dissatisfaction in buildings. *Buildings*, 15(1), 39.
Hurteau, M.D., Bradford, J.B., Fulé, P.Z., Taylor, A.H., Martin, K.L., 2014. Climate change, fire management, and ecological services in the southwestern US. For. Ecol. Manag. 327. https://doi.org/10.1016/j.foreco.2013.08.007.
Hussain, K., Mehmood, K., Anees, S.A., Ding, Z., Muhammad, S., Badshah, T., Shahzad, F., Haidar, I., Wahab, A., Ali, J., 2024. Assessing forest fragmentation due to land use changes from 1992 to 2023: A spatio-temporal analysis using remote sensing data. Heliyon 10 (14).
Iban, M.C., Aksu, O., 2024. SHAP-Driven Explainable Artificial Intelligence Framework for Wildfire Susceptibility Mapping using MODIS active Fire Pixels: An In-Depth Interpretation of contributing Factors in Izmir, Türkiye. Remote Sens. 16 (15), 2842.
Jain, P., Coogan, S.C.P., Subramanian, S.G., Crowley, M., Taylor, S., Flannigan, M.D., 2020. A review of machine learning applications in wildfire science and management. Environ. Rev. 28 (4), 478–505.
Jin, Y., Ge, Y., Fan, H., Li, Z., Liu, Y., Jia, Y., 2023. Mapping Gross domestic product distribution at 1 km Resolution across Thailand using the Random Forest Area-to-Area Regression Kriging Model. ISPRS Int. J. Geo Inf. 12 (12). https://doi.org/10.3390/ijgi12120481.
Joharestani, M.Z., Cao, C., Ni, X., Bashir, B., Talebiesfandarani, S., 2019. PM2.5 prediction based on random forest, XGBoost, and deep learning using multisource remote sensing data. Atmosphere 10 (7). https://doi.org/10.3390/atmos10070373.
Kabbilawsh, P., Kumar, D.S., Chithra, N.R., 2024. Assessment of temporal homogeneity of long-term rainfall time-series datasets by applying classical homogeneity tests. Environ. Dev. Sustain. 26 (7). https://doi.org/10.1007/s10668-023-03310-0.
Kaewsong, K., Chang-Yang, C.H., Bunyavejchewin, S., Kraichak, E., Yang, J., Sun, Z., Zhang, C., Li, W., Lin, L., Sun, I.F., 2022. Effects of fire disturbance on species and functional compositions vary with tree sizes in a tropical dry forest. PeerJ 10. https://doi.org/10.7717/peerj.13270.
Kanchanaroek, Y., Rattanakaew, T., Kako, P., Meangbua, O., Doungjun, W., 2025. Spatial-Economic Analysis of Greenhouse Gas Emissions from Agricultural Residue Burning in Thailand's Rice, Maize, and Sugarcane Cultivation Areas.
Kanjanavanit, S., 1992. Aspects of the Temporal Pattern of Dry Season Fires in the Dry Dipterocarp Forests of Thailand. University of London, School of Oriental and African Studies (United Kingdom).
Keeley, J.E., Pausas, J.G., 2022. Evolutionary Ecology of Fire. In: *Annual Review of Ecology, Evolution, and Systematics* (Vol. 53). https://doi.org/10.1146/annurev-ecolsys-102320-095612.
Kim, H.S., Kim, H.S., Choi, S.Y., 2024. Investigating the Impact of Agricultural, Financial, Economic, and Political Factors on Oil Forward prices and volatility: A SHAP Analysis. Energies 17 (5). https://doi.org/10.3390/en17051001.
Kirillina, K., Shvetsov, E.G., Protopopova, V.V., Thiesmeyer, L., Yan, W., 2020. Consideration of anthropogenic factors in boreal forest fire regime changes during rapid socio-economic development: case study of forestry districts with increasing burnt area in the Sakha Republic, Russia. Environ. Res. Lett. 15 (3). https://doi.org/10.1088/1748-9326/ab6c6e.
Knapp, E.E., Estes, B.L., Skinner, C.N., 2009. Ecological Effects of Prescribed Fire Season: A Literature Review and Synthesis for Managers. In: Gen. Tech. Rep. PSW-GTR-224. Albany, CA: U.S. Department of Agriculture, Forest Service, Pacific Southwest Research Station, September.
Kolzow, D. R., Smith, C. C. C., Serrat, O., Dilie, H. M., Zeeshan, S., Ng, S. I., Ho, J. A., Jantan, A. H., Massey, J., Sulak, T., Sriram, R., Dennis, R. S., Bocarnea, M., Hai, T. N., Van, Q. N., Herbert, S. L., So-Jung Kim, Kyoung-Seok Kim, Y.-G. C., Guillaume, O., Honeycutt, A., … Ingram, O. C.(2021). Unit 5 Theories of leadership. *Int. J. Organ. Leadersh.*, 1(1).
Kominoski, J.S., Fernandez, M., Breault, P., Sclater, V., Rothermel, B.B., 2022. Fire Severity and Post-fire Hydrology Drive Nutrient Cycling and Plant Community Recovery in Intermittent Wetlands. Ecosystems 25 (2). https://doi.org/10.1007/s10021-021-00653-5.
Konya, A., Nematzadeh, P., 2024. Recent applications of AI to environmental disciplines: A review. Sci. Total Environ. 906. https://doi.org/10.1016/j.scitotenv.2023.167705.

Kumar, V., Kedam, N., Sharma, K.V., Mehta, D.J., Caloiero, T., 2023. Advanced machine learning techniques to improve hydrological prediction: A comparative analysis of streamflow prediction models. Water 15 (14), 2572.
Kumari, S., Radhadevi, L., Gujre, N., Rao, N., Bandaru, M., 2024. Assessing the Impact of Forest Fires on Air Quality in Northeast India. Atmospheres, Environmental Science.
Kuter, S., Usul, N., Kuter, N., 2011a. Bandwidth determination for kernel density analysis of wildfire events at forest sub-district scale. Ecol. Model. 222 (17), 3033–3040.
Kuter, N., Yenilmez, F., Kuter, S., 2011b. Forest fire risk mapping by kernel density estimation. Croatian J. Forest Eng. 32 (2), 599–610.
Le, H.T., Tran, T.V., Gyeltshen, S., Nguyen, C.P.T., Tran, D.X., Luu, T.H., Duong, M.B., 2020. Characterizing spatiotemporal patterns of mangrove forests in can gio biosphere reserve using sentinel-2 imagery. Appl. Sci. (Switz.) 10 (12). https://doi.org/10.3390/APP10124058.
Lebel, L., 2009. Impacts of climate change and ADAPTATION in Thailand. In: Regional Assessments and Profiles of Climate Change Impacts and Adaptation in PRC, Thailand and Viet Nam: Biodiversity, Food Security, Water Resources and Rural Livelihoods in the GMS, 17.
Littell, J.S., Peterson, D.L., Riley, K.L., Liu, Y., Luce, C.H., 2016. A review of the relationships between drought and forest fire in the United States. In: *Global change biology* (Vol. 22, issue 7). https://doi.org/10.1111/gcb.13275.
Littidej, P., Uttha, T., Pumhirunroj, B., 2022. Spatial Predictive Modeling of the burning of Sugarcane Plots in Northeast Thailand with selection of factor Sets using a GWR Model and Machine Learning based on an ANN-CA. Symmetry 14 (10). https://doi.org/10.3390/sym14101989.
Lu, Z., Zhang, Q., Streets, D.G., 2011. Sulfur dioxide and primary carbonaceous aerosol emissions in China and India, 1996-2010. In: *Atmospheric Chemistry and Physics* (Vol. 11, issue 18). https://doi.org/10.5194/acp-11-9839-2011.
Martínez, B., Sánchez-Ruiz, S., Campos-Taberner, M., García-Haro, F.J., Gilabert, M.A., 2022. Exploring Ecosystem Functioning in Spain with Gross and net primary Production Time Series. Remote Sens. 14 (6). https://doi.org/10.3390/rs14061310.
Mehmood, K., Anees, S.A., Muhammad, S., Hussain, K., Shahzad, F., Liu, Q., Ansari, M.J., Alharbi, S.A., Khan, W.R., 2024a. Analyzing vegetation health dynamics across seasons and regions through NDVI and climatic variables. Sci. Rep. 14 (1), 1–22. https://doi.org/10.1038/s41598-024-62464-7.
Mehmood, K., Anees, S.A., Rehman, A., Rehman, N.U., Muhammad, S., Shahzad, F., Liu, Q., Alharbi, S.A., Alfarraj, S., Ansari, M.J., 2024b. Assessment of climatic influences on net primary productivity along elevation gradients in temperate ecoregions. Trees, Forests and People 18, 100657.
Mehmood, K., Anees, S.A., Shahzad, F., Muhammad, S., Liu, Q., Khan, W.R., Jamjareegulgarn, P., 2025. Exploring vegetation health in Southern Thailand under climate stress from temperature and water impacts between 2000 and 2023. Sci. Rep. 15 (1), 30491.
Michel, C., Liousse, C., Grégoire, J.M., Tansey, K., Carmichael, G.R., Woo, J.H., 2005. Biomass burning emission inventory from burnt area data given by the SPOT-VEGETATION system in the frame of TRACE-P and ACE-Asia campaigns. J. Geophys. Res. D: Atmosph. 110 (9). https://doi.org/10.1029/2004JD005461.
Moran, J., NaSuwan, C., Poocharoen, O.O., 2019. The haze problem in Northern Thailand and policies to combat it: A review. Environ. Sci. Policy 97. https://doi.org/10.1016/j.envsci.2019.03.016.
Mouillot, F., Rambal, S., Joffre, R., 2002. Simulating climate change impacts on fire frequency and vegetation dynamics in a Mediterranean-type ecosystem. Glob. Chang. Biol. 8 (5). https://doi.org/10.1046/j.1365-2486.2002.00494.x.
Murphy, B.P., Whitehead, P.J., Evans, J., Yates, C.P., Edwards, A.C., MacDermott, H.J., Lynch, D.C., Russell-Smith, J., 2023. Using a demographic model to project the long-term effects of fire management on tree biomass in Australian savannas. Ecol. Monogr. 93 (2). https://doi.org/10.1002/ecm.1564.
Mushtaq, K., Waris, A., Zou, R., Shafique, U., Khan, N.B., Khan, M.I., Jameel, M., Khan, M.I., 2024. A Comprehensive Approach to Wind Turbine Power Curve Modeling: addressing Outliers and Enhancing Accuracy. Energy 131981.
Nohara, Y., Matsumoto, K., Soejima, H., Nakashima, N., 2022. Explanation of machine learning models using shapley additive explanation and application for real data in hospital. Comput. Methods Prog. Biomed. 214. https://doi.org/10.1016/j.cmpb.2021.106584.
Permsirivanchai, J., 2017. Forest Area of Thailand, 1973–2016. Forest Land Management Bureau, Royal Forestry Department of Thailand.
Phairuang, W., Suwattiga, P., Chetiyanukornkul, T., Hongtieab, S., Limpaseni, W., Ikemori, F., Hata, M., Furuuchi, M., 2019. The influence of the open burning of agricultural biomass and forest fires in Thailand on the carbonaceous components in size-fractionated particles. Environ. Pollut. 247, 238–247.
Pichler, M., Hartig, F., 2023. Machine learning and deep learning—A review for ecologists. In: *Methods in Ecology and Evolution* (Vol. 14, issue 4). https://doi.org/10.1111/2041-210X.14061.
Podur, J., Wotton, M., 2010. Will climate change overwhelm fire management capacity? Ecol. Model. 221 (9). https://doi.org/10.1016/j.ecolmodel.2010.01.013.
Pomoim, N., Trisurat, Y., Hughes, A.C., Corlett, R.T., 2022. Can Thailand Protect 30% of its Land Area for Biodiversity, and will this be enough? Diversity 14 (5). https://doi.org/10.3390/d14050344.
Ponce-Bobadilla, A.V., Schmitt, V., Maier, C.S., Mensing, S., Stodtmann, S., 2024. Practical guide to SHAP analysis: explaining supervised machine learning model predictions in drug development. Clin. Transl. Sci. 17 (11), e70056.
Punsompong, P., Pani, S.K., Wang, S.H., Bich Pham, T.T., 2021. Assessment of biomass-burning types and transport over Thailand and the associated health risks. Atmos. Environ. 247. https://doi.org/10.1016/j.atmosenv.2020.118176.
Romanov, A.A., Tamarovskaya, A.N., Gusev, B.A., Leonenko, E.V., Vasiliev, A.S., Krikunov, E.E., 2022. Catastrophic PM2.5 emissions from Siberian forest fires: Impacting factors analysis. Environ. Pollut. 306. https://doi.org/10.1016/j.envpol.2022.119324.
Rovithakis, A., Voulgarakis, A., 2024. Wildfire aerosols and their impact on weather: A case study of the August 2021 fires in Greece using the WRF-Chem model. Atmos. Sci. Lett. e1267.
Russell-Smith, J., Yates, C., Vernooij, R., Eames, T., van der Werf, G., Ribeiro, N., Edwards, A., Beatty, R., Lekoko, O., Mafoko, J., Monagle, C., Johnston, S., 2021. Opportunities and challenges for savanna burning emissions abatement in southern Africa. J. Environ. Manag. 288. https://doi.org/10.1016/j.jenvman.2021.112414.
Seiler, W., Crutzen, P.J., 1980. Estimates of gross and net fluxes of carbon between the biosphere and the atmosphere from biomass burning. Clim. Chang. 2 (3). https://doi.org/10.1007/BF00137988.
Shahani, N.M., Zheng, X., Liu, C., Hassan, F.U., Li, P., 2021. Developing an XGBoost Regression Model for predicting Young's Modulus of Intact Sedimentary Rocks for the Stability of Surface and Subsurface Structures. Front. Earth Sci. 9. https://doi.org/10.3389/feart.2021.761990.
Shahzad, F., Mehmood, K., Hussain, K., Haidar, I., Anees, S.A., Muhammad, S., Ali, J., Adnan, M., Wang, Z., Feng, Z., 2024. Comparing machine learning algorithms to predict vegetation fire detections in Pakistan. Fire Ecol. 20 (1), 57.
Shao, Y., Feng, Z., Cao, M., Wang, W., Sun, L., Yang, X., Ma, T., Guo, Z., Fahad, S., Liu, X., 2023. An ensemble model for forest fire occurrence mapping in China. Forests 14 (4), 704.
Shi, Y., Yamaguchi, Y., 2014. A high-resolution and multi-year emissions inventory for biomass burning in Southeast Asia during 2001-2010. Atmos. Environ. 98. https://doi.org/10.1016/j.atmosenv.2014.08.050.
Shi, Y., Sasai, T., Yamaguchi, Y., 2014. Spatio-temporal evaluation of carbon emissions from biomass burning in Southeast Asia during the period 2001-2010. Ecol. Model. 272. https://doi.org/10.1016/j.ecolmodel.2013.09.021.
Shirazi, Z., Guo, H., Chen, F., Yu, B., Li, B., 2017. Assessing the impact of climatic parameters and their inter-annual seasonal variability on fire activity using time series satellite products in South China (2001–2014). Nat. Hazards 85 (3). https://doi.org/10.1007/s11069-016-2631-3.
Shuo, Z., Jingyu, Z., Zhengxiang, Z., Jianjun, Z., 2021. Identifying the density of grassland fire points with kernel density estimation based on spatial distribution characteristics. Open Geosci. 13 (1), 796–806.
Song, Z., Liu, Y., 2019. Fire intensity affects the relationship between species diversity and the N utilization stability of dominant species. Forests 10 (3). https://doi.org/10.3390/f10030207.
Sulla-Menashe, D., Friedl, M.A., 2018. User guide to collection 6 MODIS land cover (MCD12Q1 and MCD12C1) product. Usgs: Reston, Va, Usa 1, 18.
Sun, L., Feng, Z., Shao, Y., Wang, L., Su, J., Ma, T., Lu, D., An, J., Pang, Y., Fahad, S., 2023. The Development of a Set of Novel Low cost and Data Processing-Free measuring Instruments for tree Diameter at Breast Height and tree Position. Forests 14 (5), 891.
Talukdar, N.R., Ahmad, F., Goparaju, L., Choudhury, P., Qayum, A., Rizvi, J., 2024. Forest fire in Thailand: Spatio-temporal distribution and future risk assessment. Nat. Hazards Res. 4 (1). https://doi.org/10.1016/j.nhres.2023.09.002.
Taweesan, A., Lalitaporn, P., Sooktawee, S., Kanabkaew, T., 2025. Mitigating air quality and climate impact: A comprehensive analysis of paddy field burning emissions and green mechanisms for sustainable agriculture. Environ. Sustain. Indic. 26, 100662.
Taylor, D., 2010. Biomass burning, humans and climate change in Southeast Asia. Biodivers. Conserv. 19 (4). https://doi.org/10.1007/s10531-009-9756-6.
Tiwari, A., Nanjundan, P., Kumar, R.R., Soni, V.K., 2024. A framework for natural resource management with geospatial machine learning: a case study of the 2021 Almora forest fires. Fire Ecol. 20 (1), 78.
Tripathi, S.N., Yadav, S., Sharma, K., 2024. Air pollution from biomass burning in India. Environ. Res. Lett. 19 (7), 073007.
Unger, N., Shindell, D.T., Koch, D.M., Amann, M., Cofala, J., Streets, D.G., 2006. Influences of man-made emissions and climate changes on tropospheric ozone, methane, and sulfate at 2030 from a broad range of possible futures. J. Geophys. Res. Atmos. 111 (12). https://doi.org/10.1029/2005JD006518.
UU Republik Indonesia, Munawir, M., Nasional, B. S., Susanta, G., Jatimnet.com, MajaMojokerto.net, Radarmojokerto.jawapos.com, Wijayakusuma, D. M. S., Nahman, A., Godfrey, L., Jacobsen, R., Buysse, J., Gellynck, X., Bayu, D., Depkes, R., Soekidjo Notoatmodjo, Boulanger, L., Ismoyo, I. H., Tarigan, R., … Sanyal, S. (2022). Penentuan alternatif lokasi tempat pembuangan akhir (tpa) sampah di kabupaten sidoarjo. Energies, 15(1).
Van der Werf, G.R., Randerson, J.T., Collatz, G.J., Giglio, L., 2003. Carbon emissions from fires in tropical and subtropical ecosystems. Glob. Chang. Biol. 9 (4). https://doi.org/10.1046/j.1365-2486.2003.00604.x.
Van Der Werf, G.R., Randerson, J.T., Giglio, L., Collatz, G.J., Mu, M., Kasibhatla, P.S., Morton, D.C., Defries, R.S., Jin, Y., Van Leeuwen, T.T., 2010. Global fire emissions and the contribution of deforestation, savanna, forest, agricultural, and peat fires (1997-2009). Atmos. Chem. Phys. 10 (23). https://doi.org/10.5194/acp-10-11707-2010.
Wang, L., Lu, Y., Wang, Z., Li, H., Zhang, M., 2024. Hourly solar radiation estimation and uncertainty quantification using hybrid models. Renew. Sust. Energ. Rev. 202, 114727.
Wang, Y., Tian, Y., Shi, Y., 2025. Estimation of Biomass Burning Emissions in South and Southeast Asia Based on FY-4A Satellite Observations. Atmosphere 16 (5), 582.
Ward, D.E., Hardy, C.C., 1991. Smoke emissions from wildland fires. Environ. Int. 17 (2–3). https://doi.org/10.1016/0160-4120(91)90095-8.
Williams, C.A., Collatz, G.J., Masek, J., Goward, S.N., 2012. Carbon consequences of forest disturbance and recovery across the conterminous United States. Glob. Biogeochem. Cycles 26 (1). https://doi.org/10.1029/2010GB003947.

Xi, Z., Chen, G., Xing, Y., Xu, H., Tian, Z., Ma, Y., Cui, J., Li, D., 2023. Spatial and temporal variation of vegetation NPP and analysis of influencing factors in Heilongjiang Province, China. Ecol. Indic. 154. https://doi.org/10.1016/j.ecolind.2023.110798.

Yin, S., 2020. Biomass burning spatiotemporal variations over South and Southeast Asia. Environ. Int. 145. https://doi.org/10.1016/j.envint.2020.106153.

Yu, Q., Hou, Z., Wang, Z., 2024. Predictive modeling of preoperative acute heart failure in older adults with hypertension: a dual perspective of SHAP values and interaction analysis. BMC Med. Inform. Decis. Mak. 24 (1), 329.

Zhan, X., Ma, Y., Huang, Z., Zheng, C., Lin, H., Tigabu, M., Guo, F., 2023. Temporal and spatial dynamics in emission of water-soluble ions in fine particulate matter during forest fires in Southwest China. Front. Forest. Global Change 6. https://doi.org/10.3389/ffgc.2023.1250038.

Zhang, Z., Feng, Z., Zhang, H., Zhao, J., Yu, S., Du, W., 2017. Spatial distribution of grassland fires at the regional scale based on the MODIS active fire products. Int. J. Wildland Fire 26 (3), 209–218.

Zhang, L., Zhou, D., Fan, J., Guo, Q., Chen, S., Wang, R., Li, Y., 2019. Contrasting the performance of eight satellite-based GPP models in water-limited and temperature-limited grassland ecosystems. Remote Sens. 11 (11). https://doi.org/10.3390/rs11111333.

Zhang, Z., Wang, L., Xue, N., Du, Z., 2021. Spatiotemporal analysis of active fires in the Arctic region during 2001–2019 and a fire risk assessment model. Fire 4 (3), 57.

Zhang, Y., Liu, J., Shen, W., 2022. A review of ensemble learning algorithms used in remote sensing applications. In: *Applied Sciences (Switzerland)* (Vol. 12, issue 17). https://doi.org/10.3390/app12178654.

Zhang, W., Yang, Y., Hu, C., Zhang, L., Hou, B., Wang, W., Li, Q., Li, Y., 2023. NPP and Carbon Emissions under Forest Fire Disturbance in Southwest and Northeast China from 2001 to 2020. Forests 14 (5). https://doi.org/10.3390/f14050999.

Zhao, Y., Wang, C., Wang, S., Tibig, L.V., 2005. Impacts of present and future climate variability on agriculture and forestry in the humid and sub-humid tropics. In: Increasing Climate Variability and Change. Reducing the Vulnerability of Agriculture and Forestry. https://doi.org/10.1007/1-4020-4166-7_5.